

Quasibiennial oscillation in tropical ozone as revealed by ozonesonde and satellite data

J. A. Logan,¹ D. B. A. Jones,¹ I. A. Megretskaya,¹ S. J. Oltmans,² B. J. Johnson,² H. Vömel,² W. J. Randel,³ W. Kimani,⁴ and F. J. Schmidlin⁵

Received 5 February 2002; revised 22 November 2002; accepted 11 December 2002; published 23 April 2003.

[1] We present an analysis of the quasi-biennial oscillation (QBO) in tropical ozone using recent in situ measurements made by ozonesondes, supplemented by satellite profile and column data. The first in situ equatorial ozone profiles reveal the dramatic change in shape of the profile that accompanies the descent of the westerly shear zone. The partial pressure maximum in ozone increases by $\sim 25\%$ in 5–6 months as it descends from 17.5 to 24 hPa. The amplitude of the QBO anomaly that extends from 15 to 80 hPa is found to exceed $\pm 20\%$, larger than indicated by earlier analyses of satellite data. The influence of the QBO on equatorial ozone is dominant between 10 and 45 hPa, but the seasonal cycle is more important below 50 hPa. The equatorial ozone anomalies are influenced by El Niño–Southern Oscillation (ENSO) in the lowest part of the stratosphere. The ozone anomaly in the lower stratosphere at 20°S lags that at the equator by only a few months during the easterlies from 1994 to 1998, contrary to the previous picture of the subtropical and equatorial anomalies being out of phase. There is often a three-cell structure in ozone anomalies at 20°N and 20°S , with the upper two related to the QBO and that below 50 hPa sometimes related to ENSO. We present an analysis of the contribution of the ozone anomalies as a function of altitude to the subtropical QBO in column ozone. There is a strong subtropical column anomaly (>5 Dobson units (DU)) when the anomalies above 20 hPa and from 50 to 20 hPa reinforce. There were four such cases at 20°N and at 20°S in 1985–1991, but five at 20°N and only one at 20°S in 1993–1999. About 70% of these cases are associated with strong shear at 25–35 hPa in late fall/early winter. There is a weak subtropical anomaly in column ozone when the ozone anomalies above and below 20 hPa are of opposite sign, or one of them is very weak. Over half of these cases are associated with strong wind shear in late fall/early winter in the middle stratosphere at 12.5 hPa. In the southern subtropics, there is strong shear at 12.5 hPa and a weak column ozone anomaly for 5 of 6 years from 1994 to 1999. Near 20°N the seasonal cycle contributes more to the ozone variance above 20 hPa than does the QBO, but the reverse appears true near 20°S . The seasonal cycle dominates the variance in ozone below 40 hPa at 20°S . The effects of ENSO are more important for ozone than those of the QBO below 60 hPa at 20°N .

INDEX TERMS: 0340 Atmospheric Composition and Structure: Middle atmosphere—composition and chemistry; 0341 Atmospheric Composition and Structure: Middle atmosphere—constituent transport and chemistry (3334); 0399 Atmospheric Composition and Structure: General or miscellaneous; **KEYWORDS:** quasibiennial oscillation, QBO, stratospheric ozone, SHADOZ, SAGE, ozonesonde

Citation: Logan, J. A., D. B. A. Jones, I. A. Megretskaya, S. J. Oltmans, B. J. Johnson, H. Vömel, W. J. Randel, W. Kimani, and F. J. Schmidlin, Quasibiennial oscillation in tropical ozone as revealed by ozonesonde and satellite data, *J. Geophys. Res.*, 108(D8), 4244, doi:10.1029/2002JD002170, 2003.

¹Department of Earth and Planetary Sciences, Harvard University, Cambridge, Massachusetts, USA.

²Climate and Diagnostic Laboratory, NOAA, Boulder, Colorado, USA.

³National Center for Atmospheric Research, Boulder, Colorado, USA.

⁴Kenya Meteorological Department, Nairobi, Kenya.

⁵NASA Wallops Flight Facility, Wallops Island, Virginia, USA.

1. Introduction

[2] We describe here recent in situ measurements of equatorial ozone which reveal the dramatic effect of the quasi-biennial oscillation (QBO) on the shape of the vertical profile. We then present a detailed analysis of the QBO in tropical ozone using recent ozonesonde measurements supplemented by satellite observations. The QBO is a downward propagating oscillation between easterly and westerly

wind regimes in the equatorial stratosphere, with a mean period of about 28 months [e.g., *Reed et al.*, 1961; *Baldwin et al.*, 2001]. Associated with the oscillation in the winds is an oscillation in temperature. The amplitudes of these oscillations are highest over the equator, and they drop off rapidly with increasing latitude. The QBO is caused by the interaction of waves propagating up from the troposphere with the zonal-mean equatorial stratospheric wind [*Lindzen and Holton*, 1968; *Holton and Lindzen*, 1972; *Dunkerton*, 1997]. *Baldwin et al.* [2001] give a comprehensive review of all aspects of the QBO, including effects on the transport of trace gases.

[3] The interannual variability in equatorial ozone is dominated by a quasi-biennial signal, as shown by analyses of satellite measurements of the ozone column [e.g., *Bowman*, 1989; *Hollandsworth et al.*, 1995; *Randel and Wu*, 1996], and earlier analyses of ground-based column measurements [e.g., *Oltmans and London*, 1982]. These studies showed that the ozone column variations within 10° of the equator are approximately in phase with the equatorial winds near 30 hPa, while the extratropical variations are of opposite phase, with the phase change near 10° – 15° . The QBO signal in the vertical distribution of equatorial ozone has been examined with data from the Stratospheric Aerosol and Gas Experiment (SAGE) [*Zawodny and McCormick*, 1991; *Hasebe*, 1994; *Randel and Wu*, 1996]. These studies show positive and negative ozone anomalies which propagate downwards with time; the anomalies are located at 20–27 km (55–20 hPa) and 30–37 km (12–4.5 hPa), with a phase change near 29 km.

[4] The vertical structure of the QBO signal in ozone is influenced by the photochemical lifetime of ozone, as first illustrated by the simulations of *Ling and London* [1986]. The lifetime for odd-oxygen increases with decreasing altitude; it is about 10 days at 34 km, 5 weeks at 30 km, and 3 months at 27 km, based on the model of *Jones et al.* [1998]; similar lifetimes are shown by *Garcia and Solomon* [1985]. In the lower stratosphere ozone can be considered as a long-lived tracer, and the QBO structure is generated by vertical transport. *Reed* [1964] argued that there is a meridional circulation driven by the temperature QBO, which is symmetric about the equator and changes phase near $\pm 15^\circ$. The QBO in temperature is in thermal wind balance with the vertical gradient, or shear, of the zonal winds in the equatorial zone. The temperature structure is maintained against radiative damping by adiabatic heating or cooling. At the time of maximum westerly shear at a given altitude, temperatures are highest, and there is maximum radiative cooling; this is balanced by relative subsidence over the equator and rising motions in the subtropics. Since the ozone mixing ratio increases from 100 hPa to ~ 10 hPa (Figure 1), the relative downward motion over the equator causes an increase in ozone at a given altitude and a positive ozone anomaly, while the relative upward motion in the subtropics causes a negative ozone anomaly. In the easterly shear zone the temperatures are coolest, causing minimum radiative cooling which is balanced by relative upward motion over the equator and sinking in the subtropics, resulting in negative ozone anomalies over the equator and positive ozone anomalies in the subtropics.

[5] The ozone lifetime is controlled largely by photochemistry above 30 km, with the catalytic cycle involving

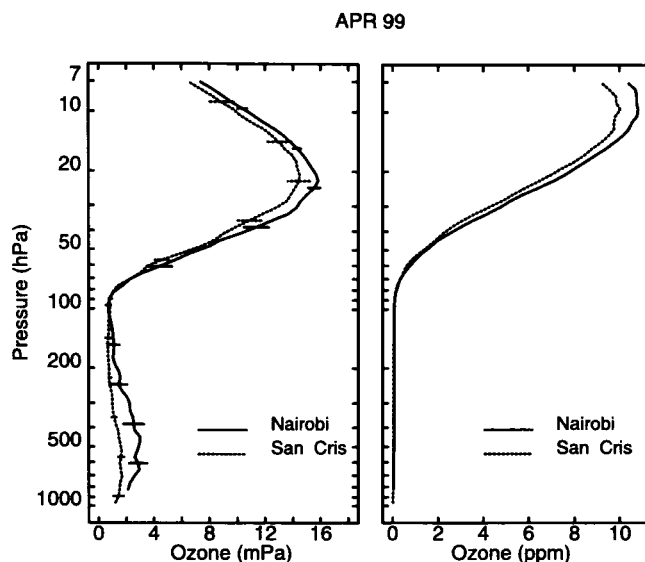


Figure 1. Monthly mean ozonesonde profiles for March, 1998, for Nairobi (solid) and San Cristobal (dashed). The left panel shows the ozone partial pressure in mPa, the right panel shows the ozone mixing ratio in ppm. The horizontal lines show the mean ± 2 standard errors.

NO_x playing a major role. In this region the QBO in ozone is caused by dynamically induced variations in NO_y [*Chipperfield et al.*, 1994], which are responsible for the QBO that is observed in NO_2 [*Zawodny and McCormick*, 1991]. The mixing ratio of NO_y in the tropical lower stratosphere increases with altitude and decreases with latitude. Consequently, the anomalous meridional circulation associated with easterly shear, for example, will produce a decrease in the abundance of NO_y and thus NO_2 in the equatorial middle stratosphere. This in turn will result in a positive ozone anomaly, as the rate of NO_x -mediated catalytic ozone loss will decrease. In the subtropical middle stratosphere the circulation anomaly will produce an increase in NO_y and NO_2 , and so a negative ozone anomaly as the rate of NO_x -mediated catalytic ozone loss increases.

[6] We present here an analysis of recent ozonesonde measurements from the tropics, with a focus on analysis of the effect of the QBO on the ozone profiles. Measurements from Nairobi, Kenya (1°S , 37°E), and San Cristobal, Galapagos (1°S , 90°W), are unique in that they provide the first in situ profiles for ozone within 1° of the equator. The Nairobi data are most useful for examination of the QBO in equatorial ozone, as there are weekly measurements from September, 1997, to the present with few gaps. Data are available for San Cristobal for March and April, 1998, and from September, 1998, to the present. We use data from Ascension Island (8°S , 14°W), Samoa (14°S , 171°W), Tahiti (18°S , 149°W), and Fiji (18°S , 178°E) to examine the latitudinal gradient in the QBO signal in the southern tropics. The sonde stations are part of the Southern Hemisphere Additional Ozonesonde program (SHADOZ) [*Thompson et al.*, 2003]; San Cristobal is also part of the Soundings of Ozone and Water in the Equatorial Region (SOWER) program [*Fujiwara et al.*, 2001]. We did not consider data from Natal (6°S , 36°W) or Watukosek (8°S ,

112°E), as the measurements are too infrequent to be useful for this study. Data from Hilo, Hawaii (20°N, 155°W), described by *Hofmann et al.* [1993] are used to compare the QBO signal in the northern subtropics with that in the southern subtropics. Long-term data for other northern tropical stations are lacking.

[7] An advantage of the sonde data over SAGE II data for examination of the equatorial QBO is the weekly frequency of measurement. SAGE II makes measurements from 2.5°N to 2.5°S about 12 times a year, usually obtaining 9–15 profiles each time at different longitudes [*McCormick et al.*, 1989]. The measurement frequency is irregular, with gaps typically of 4–5 weeks, but with a range of a few days to 4 months. Since 1994 there has been a gap of 9 weeks between June and August, and between December and February, except in 1998/99 when the gap was 16 weeks. SAGE II data however provide larger spatial coverage and a longer time series than do the sondes. We take advantage of this below, using an extension of the analysis of *Randel and Wu* [1996] which used data prior to the eruption of Pinatubo in June, 1991.

[8] The data used here and its analysis are described in section 2. The vertical structure of the QBO signatures in the sonde and SAGE II data is presented in section 3. In section 4 we provide a detailed analysis of the contribution of the ozone anomalies as a function of altitude to the subtropical QBO signatures in column ozone. The contribution of the seasonal cycle and the QBO to the variance of ozone is described in section 5. The paper concludes with a summary and discussion in section 6.

2. Data Analysis

[9] The data discussed here were obtained with electrochemical concentration cell (ECC) ozonesondes. Temperatures were recorded with a radiosonde that is flown with the package. The various stations did not use ozonesondes from the same manufacturer, the same concentration of potassium iodide (KI), or the same pump correction efficiencies, which may result in systematic differences in ozone concentrations of several percent in the stratosphere, particularly above 20 km; this is discussed in detail by *Johnson et al.* [2002]. The procedures used at each station are described by *Thompson et al.* [2003]. A uniform set of procedures was used at San Cristobal, and at Samoa, Tahiti, and Fiji since May, 1998 [*Oltmans et al.*, 2001]. Prior to May 1998, a different concentration of KI and a different pump correction factor were used at the last three stations; this results in ozone concentrations above 20 km being a few percent larger for the earlier period than for the later period [*Johnson et al.*, 2002]. Data for the SHADOZ stations for 1998–2001 are available from <http://croc.gsfc.nasa.gov/shadoz/index.html>; data for Samoa, Tahiti, and Fiji for 1995–1997 are available from <http://www-gte.larc.nasa.gov>; and data for Hilo are available from <http://www.tor.ec.gc.ca>. Data for Nairobi in 1997 were provided by B. Hoegger (personal communication, 1999).

[10] The sonde data have not been normalized to ozone column measurements except for those from Hilo. Only a few of the SHADOZ stations have ground-based column measurements that are often used for such normalization

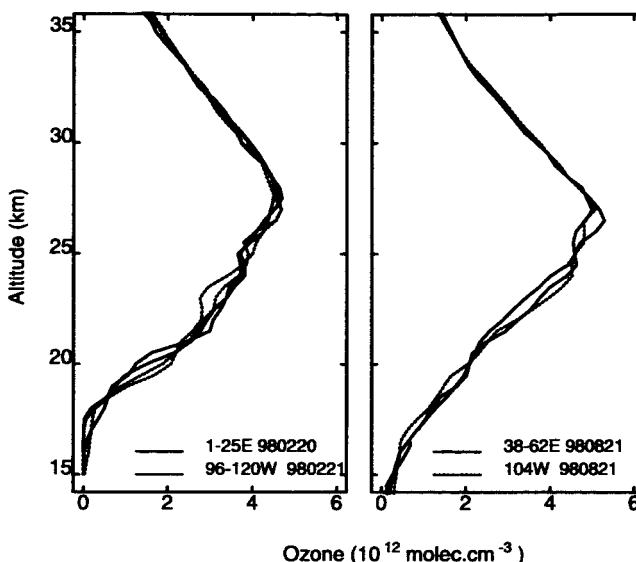


Figure 2. Profiles of ozone measured by SAGE II on February 20–21, 1998 (left) and on August 21, 1998 (right) near the longitudes of Nairobi (37°E) (solid lines) and San Cristobal (90°W) (dashed lines).

[*Thompson et al.*, 2003]. For Hilo the mean normalization, or correction, factor is 1.06, indicating that the sondes give a slightly smaller ozone column than do the ground-based measurements. Profiles with correction factors outside the range 0.8–1.2 were excluded from further analysis.

[11] The sondes provide data to about 7–8 hPa, where the balloon bursts. We integrated the SHADOZ sonde profiles using the SBUV climatology [*McPeters et al.*, 1997] above 8 hPa (or balloon burst, if at higher pressure), and made comparisons with TOMS overpass data as a check on data quality. Differences between the sonde and TOMS columns, relative to TOMS, were 3% for Nairobi, 9% for San Cristobal, Tahiti, and Fiji, 7% for Samoa, and 8% for Ascension Island, with the sondes lower than the TOMS for each location. The difference between the sonde column and the TOMS column for Samoa, Tahiti, and Fiji, was smaller, 5–6% before May 1998 than after, 9–11%, even though the originators of these data have attempted to make a homogeneous time series. There does not appear to be a jump in the time series of the ratio at the date when procedures changed (not shown). For Nairobi, the difference between the sonde column and the TOMS column was 5% prior to September, 1998, and 2.75% thereafter.

[12] A consequence of the differences in solution strength, pump correction factors, manufacturers, and procedures is that values of ozone measured above about 50 hPa at San Cristobal are systematically lower than those measured at Nairobi, as shown in Figure 1 (see also Figure 6 below); these differences exceed one standard error of the mean above ~30 hPa. These differences do not appear to be geophysical, which we confirmed by comparing equatorial SAGE II profiles near both locations. Figure 2 shows that there is no apparent longitudinal difference between the SAGE profiles near Nairobi and those near San Cristobal. The SAGE data are plotted as number density versus altitude, the natural units in which they are measured. For

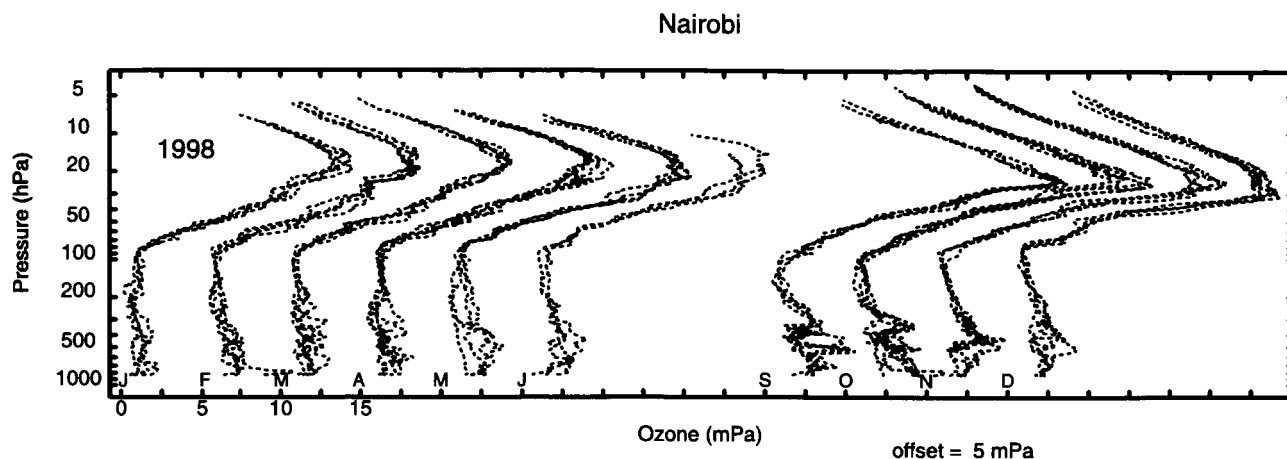


Figure 3. Individual soundings of ozone measured by ECC sondes over Nairobi in 1998. The profiles for each month after January are offset from those for the previous month by 5 mPa.

comparisons of SAGE and sonde data shown below, the sonde data were converted to number density using the temperature profiles measured concurrently with ozone.

[13] The sonde profiles were provided every 50 m, but the actual vertical resolution of the data is 150 m [World Meteorological Organization (WMO), 1998]. The data were averaged into layers of ~ 0.5 km in pressure altitude, with 60 layers equally spaced in log-pressure between 1000 and 10 hPa. A few profiles were omitted from further analysis because the difference between the sonde column and the TOMS column exceeded 20%. Monthly means for each level were formed for use in much of the analysis. Many results are shown below as monthly ozone anomalies. These were calculated for the sonde and column data by subtracting the average monthly mean over the entire record for each calendar month from the monthly mean time series (e.g., subtracting the mean of all the Januaries from the value for a particular January).

[14] The SAGE II data are Version 6.0, obtained from <http://www-sage2.larc.nasa.gov>. The stratospheric ozone data are very similar to V6.1, released in late 2001 (J. Zawodny, personal communication, 2001); ozone in V6.1 shows excellent agreement with coincident sonde data down to the tropopause [Wang et al., 2002]. The data were provided every 0.5 km, but the actual vertical resolution is about 0.75 km (J. Zawodny, personal communication, 2002); the data were sampled every 1 km for the QBO analysis. The SAGE measurements for ozone were filtered for contamination by aerosols from the Pinatubo eruption, resulting in a gap of up to 2.5 y after June, 1991, below 28 km [WMO, 1998; Cunnold et al., 2000]. Data are lacking also for the last half of 2000, because of instrument failure [Wang et al., 2002]. There are 2 months of missing data each year in the 1980s over the equator, but 3–6 months per year are missing during the 1990s. Data are missing for only 1–2 months per year in the subtropics. Monthly anomalies were calculated by fitting the irregularly sampled data to annual and semiannual harmonics, and subtracting the seasonal harmonic fits as described by Randel and Wu [1996].

[15] The ozone column data used below were obtained from http://code916.gsfc.nasa.gov/Data_services/merged/

index.html. This data set was derived by merging measurements from Nimbus 7 TOMS (Total Ozone Mapping Spectrometer), EPTOMS (Earth Probe TOMS), and SBUV (Solar Backscattered Ultraviolet) (R. S. Stolarski, personal communication, 2001). We used zonal means provided with resolution of 5° and 2° in latitude.

[16] Equatorial winds used in the analysis below are the monthly mean zonal wind component for Singapore (1°N) provided by B. Naujokat (personal communication, 2001) and Naujokat [1986]. The data are available for seven levels from 10 to 70 hPa prior to 1987, and for fourteen levels from 10 to 90 hPa for 1987 and later years.

3. Results

3.1. Ozone Near the Equator

[17] Individual profiles for ozone at Nairobi in 1998 are shown in Figure 3. Results are shown in partial pressure rather than as mixing ratio (1) to emphasize the lower stratosphere, and (2) because the integral of the ozone partial pressure versus the logarithm of pressure is proportional to the ozone column. Figure 3 shows that the variance in stratospheric ozone within any given month is rather small. There is however a dramatic change in the shape of the ozone profiles, from a rounded ozone maximum in the first half of 1998 to much more 'pointed' maxima in September to November, 1998; the profiles then start to evolve back to a more rounded shape. The rounded shape is more typical of the ozone profiles found at tropical sites such as Natal (6°S) and Samoa (14°) [e.g., Logan, 1999]. The dramatic change in shape of the profiles is caused by the QBO.

[18] The time evolution of the Nairobi ozone profiles is superimposed on the zonal component of the Singapore winds in Figure 4. The sonde data encompass one complete QBO cycle of easterly and westerly winds, and much of the next easterly phase. The QBO cycle starting in 1997 is shorter than the typical cycle, lasting only 24 months at 20 hPa; the easterly phase lasts 12 months, considerably shorter than the mean length of 18 months [Baldwin et al., 2001, Figure 1], while the westerly phase is of average length. The second easterly phase is of more typical length,

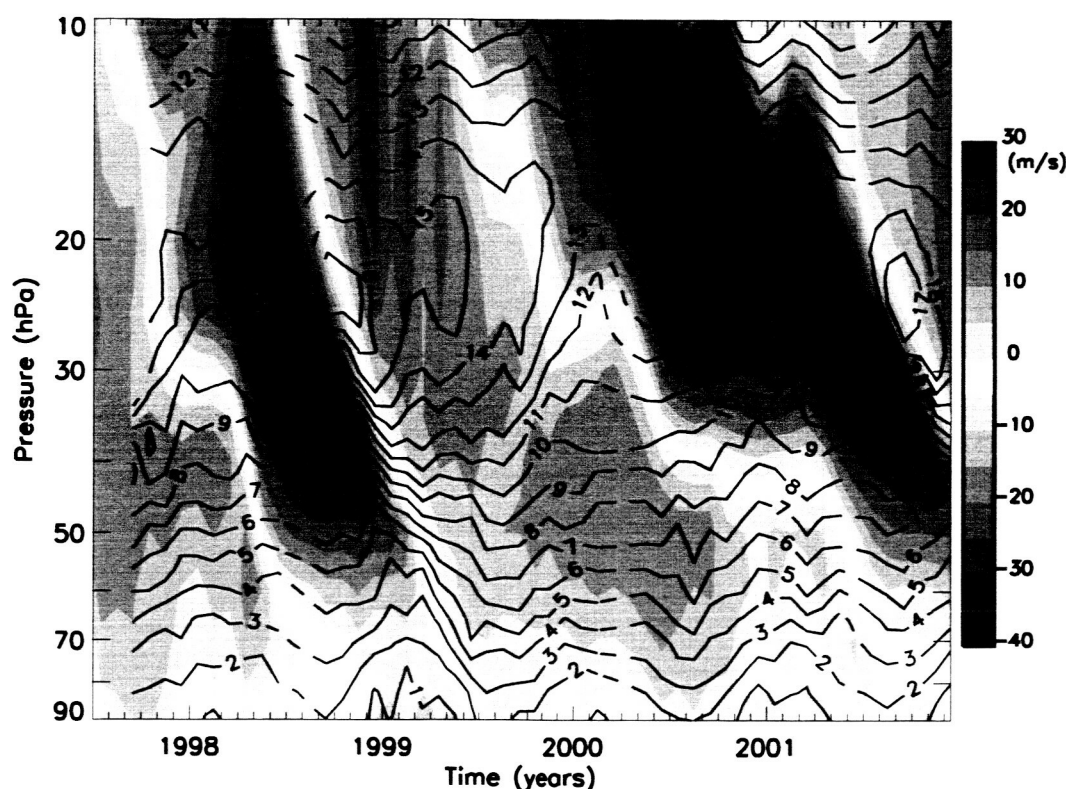


Figure 4. Contour map of ozone partial pressure (in mPa) for Nairobi superimposed on the monthly zonal wind component for Singapore, in color. Dashed lines show interpolated results. See color version of this figure at back of this issue.

21 months, with the winds becoming westerly near 20 hPa in summer of 2001.

[19] In interpreting Figure 4, it is useful to note that the QBO is the most important cause of temporal variability in ozone near the partial pressure maximum, 15 to 30 hPa, while the annual cycle is the dominant cause of temporal variability below about 60 hPa, as discussed further in section 5. Figure 4 shows that, from 20 to 35 hPa, ozone concentrations are decreasing in late 1997 in the easterly shear zone where there is relative upward motion induced by the QBO. Ozone then increases after the passage of the maximum easterly shear, with the largest increase accompanying the descent of the westerly shear zone, down to about 50 hPa, in late 1998/early 1999. The ozone maximum is about 14 mPa at 16 hPa for the first half of 1998 and increases to over 17 mPa and descends to 23 hPa in September–October, 1998, a consequence of the relative downward motion during the time of maximum westerly shear. Values of ozone at the ozone maximum then decrease and the altitude of the maximum increases to above 20 hPa, throughout the period of westerlies and the descent of the second easterly shear zone. The easterly regime stalls in mid-2000 for almost a year. Ozone increases rapidly in mid-2001 as the next westerly shear zone descends, and the earlier pattern repeats.

[20] Time series of ozone and temperature for Nairobi are shown for selected levels in Figure 5. Ozone and temperature are highly correlated between about 20 and 95 hPa. The thermal tropopause over Nairobi is located near 95 hPa from December to May and near 105 hPa from

July to September [Randel *et al.*, 2000]. The approximately in-phase relationship between ozone and temperature in the lower stratosphere was predicted by models of the equatorial QBO [Ling and London, 1986]. Around 13 hPa, where ozone is influenced more by photochemistry, the relationship between ozone and temperature is less coherent, and at higher altitudes, near 8 hPa, there is evidence of an anti-correlation. Figure 5 shows that a QBO signal is readily apparent in both ozone and temperature from 21 hPa to 52 hPa, and that the seasonal cycle dominates the time series in the lowest part of the stratosphere. The amplitude of the temperature signal in the region where the QBO dominates is 4–6 K, similar to the amplitude of the seasonal cycle from 70 to 95 hPa, as shown previously for radiosonde data by Reid [1994]. SAGE data show that the QBO in the ozone profile changes phase near 29 km (14 hPa), and the sonde data appear consistent with this, as there is not much indication of a QBO signal at 13 hPa, and the weak signal at 8 hPa is out of phase with the clear signal below 13 hPa.

[21] The ozone time series for Nairobi, San Cristobal, and Ascension are compared in Figure 6 in partial pressure and in Figure 7 as monthly anomalies. The measurements from the two equatorial stations are fairly similar, with concentrations at San Cristobal a few percent lower than those at Nairobi above the ozone maximum, but this is mainly an instrumental artifact, as discussed in section 2. The time series of ozone anomalies for these two stations are very similar in the stratosphere, but not in the upper troposphere (not shown). Ozone values at Ascension, located 8° from

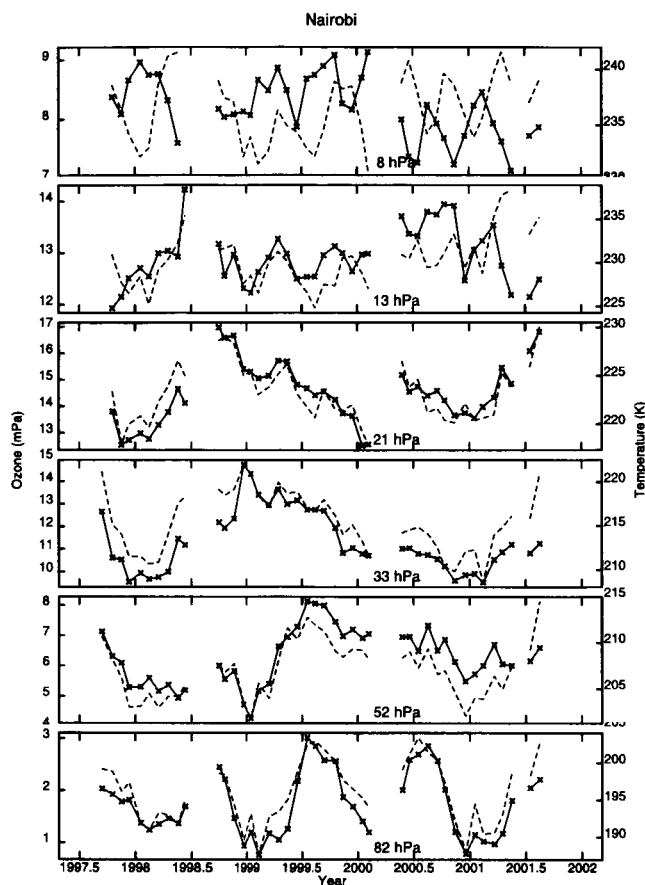


Figure 5. Time series of monthly mean values for ozone (solid, left scale) and temperature (dashed, right scale) over Nairobi. Results are shown for pressure levels that are ~ 3 km apart. The year marks denote January 1 of the given year.

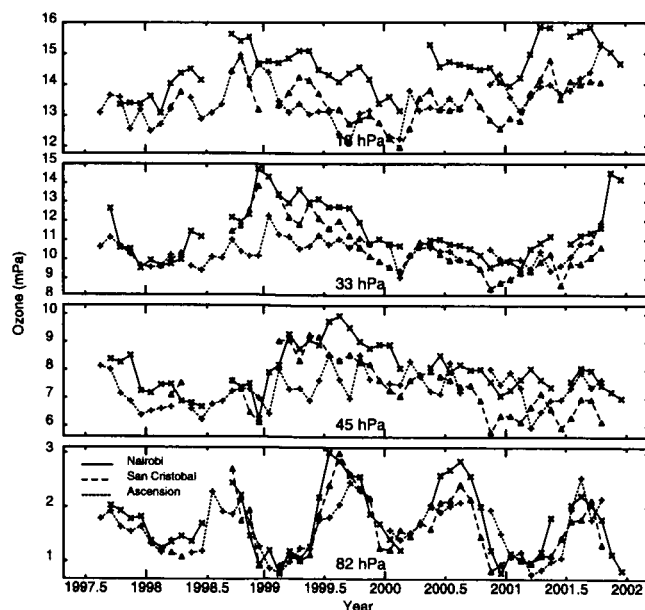


Figure 6. Time series of monthly mean values for ozone in mPa over Nairobi (solid, crosses), San Cristobal (dashed, triangles), and Ascension Island (dotted, plus).

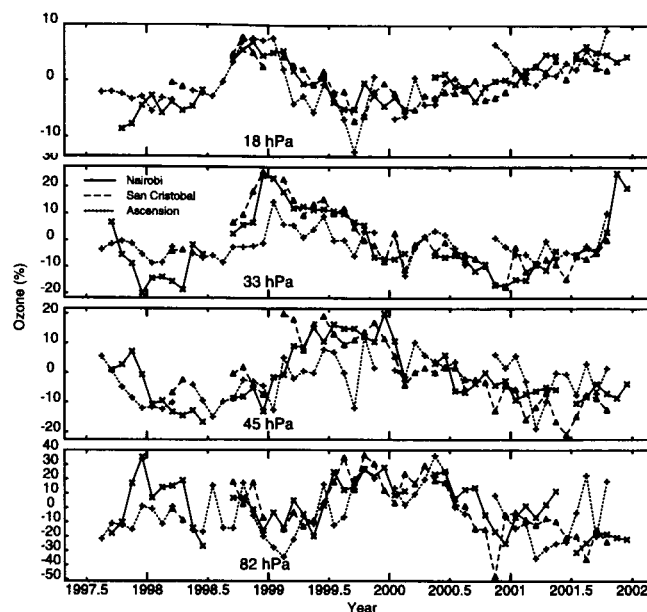


Figure 7. Time series of monthly anomalies for ozone in percent over Nairobi (solid, crosses), San Cristobal (dashed, triangles), and Ascension Island (dotted, plus).

the equator, did not increase as much in 1998 as at the two other stations during the descent of the westerly shear zone, and the monthly anomalies have a smaller amplitude than those for the equatorial stations, at least near the ozone partial pressure maximum. The QBO signal in column ozone decreases rapidly away from the equator, so it is to be expected that the amplitude of the QBO signal in the monthly anomalies is smaller for Ascension than for the equatorial stations.

[22] The monthly anomalies for Nairobi and San Cristobal are shown as contour plots in Figure 8, superimposed on the zonal component of the Singapore winds. There is a two-cell structure in the ozone anomalies, but the upper anomalies are not well resolved by the sonde data as not all profiles reach high enough. A narrow band of positive anomalies that is associated with the westerly shear zone descends from about 15 hPa in mid-1998 to 80 hPa in mid-2000; it is followed by a broad band of negative anomalies associated with the easterly shear zone, that descends from 15 hPa in mid-1999 and is still negative in late 2001, below 40 hPa. The negative anomalies are strongest in late 2000 at 30 hPa, after the easterly shear zone descends through this level after stalling near 25 hPa in early 2000. In mid-2001 another positive band of anomalies starts its descent from 15 hPa, following the descent of the westerly shear zone. The amplitude of the equatorial QBO signal is $\pm 10\%$ near 20 hPa and $\pm 15\%$ to $\pm 20\%$ from 25 to 80 hPa. Smaller amplitudes were found in the SAGE II data for 1985–1990, with a maximum amplitude of $\pm 10\%$ near 25 km (~ 25 hPa), decreasing towards 20 km [Zawodny and McCormick *et al.*, 1991]. Hasebe [1994] and Randel and Wu [1996] show equatorial anomalies in ppmv and DU/km respectively; if we assume a mean mixing ratio of 5.2 ppmv for 25 km, these studies gave anomalies of ± 7 – 10% . The QBO anomalies in the sonde data are larger likely because the stations are located almost on the equator,

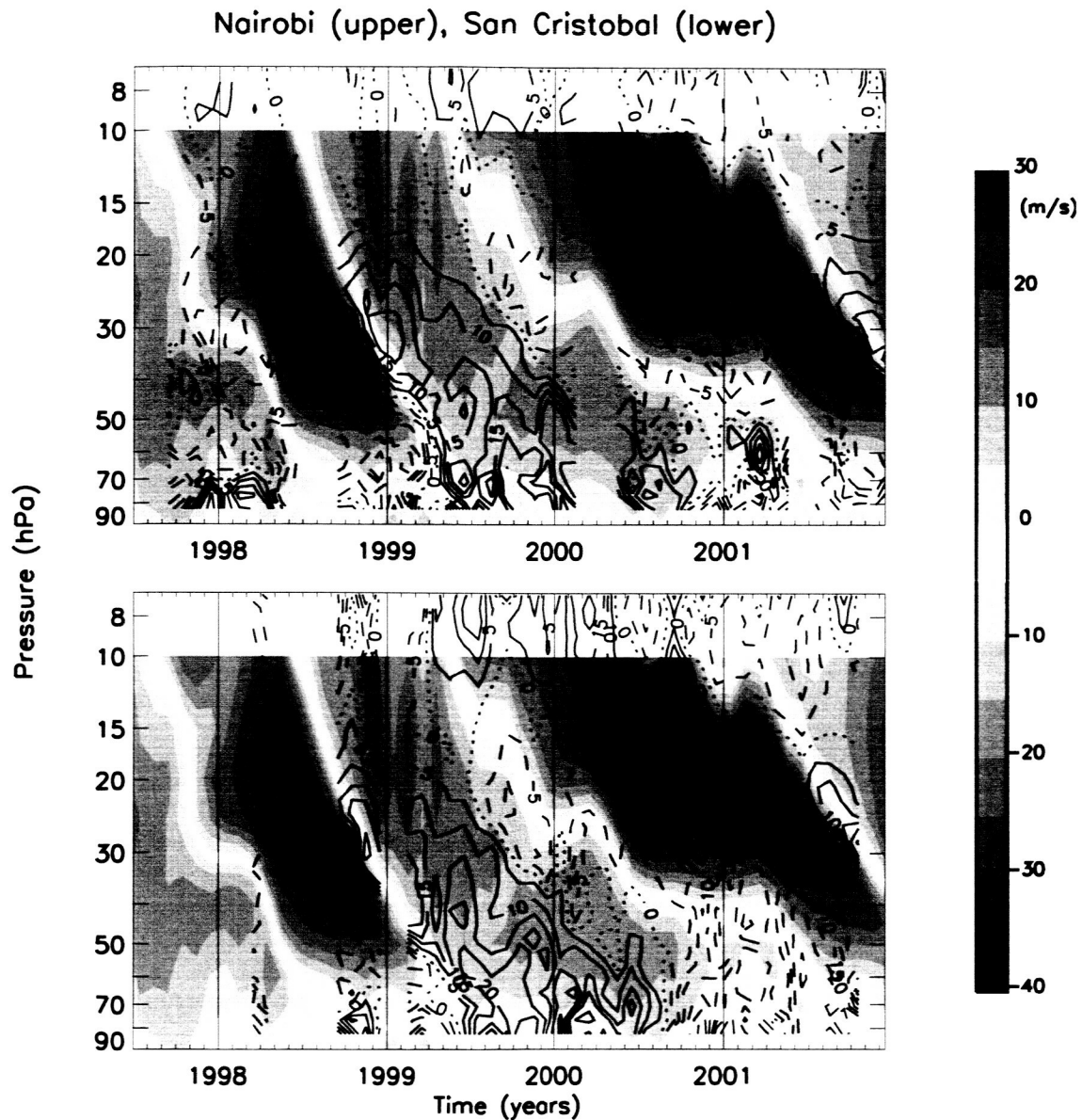


Figure 8. Contour map of monthly anomalies for ozone in percent over Nairobi, contoured by $\pm(5, 10, 15, 20, 30, 40)$. Positive contours are solid, the zero contour is dotted, and negative contours are dashed. The monthly zonal wind component for Singapore is shown in color. See color version of this figure at back of this issue.

while the older SAGE analyses averaged over several degrees of latitude.

[23] A time-height contour plot of ozone anomalies for 2°N – 2°S derived from SAGE II data is shown in Figure 9; this is an extension of the earlier analysis of *Randel and Wu* [1996], but for a narrower latitude band. The anomalies are given in units of DU km, as in the original study. Comparison of Figures 8 and 9 shows good qualitative agreement between sonde and SAGE anomalies. The SAGE II anomalies at 25 km are typically 10–15% and about –10%, slightly smaller than those derived from the sonde data. They are larger than those shown for 10°N – 10°S in the work of *Randel and Wu* [1996] because of the narrow latitude band.

[24] The SAGE II measurements reproduce the sonde profiles in the equatorial region rather well, as shown in

Figure 10, if one allows for the systematic differences between sonde data from San Cristobal and Nairobi discussed in section 2. The figure shows four of seven cases in 1998 when sonde profiles from Nairobi and San Cristobal and SAGE profiles were available with overlap criteria of 3 days, 2.5° in latitude and 35° in longitude. Previous studies of the ozone QBO using SAGE II data relied on earlier versions of the retrieval algorithm. *Wang et al.* [2002] show that SAGE II data V6.1 (very similar to V6.0 used here), agree with coincident sonde data from 30 km to the tropopause, usually within 5%; earlier versions showed differences exceeding 10% below 20 km [WMO, 1998]. Thus it is expected that the SAGE II data and the sonde data should now give consistent results for the QBO signal in the lower stratosphere.

SAGEII ozone anomalies EQTR

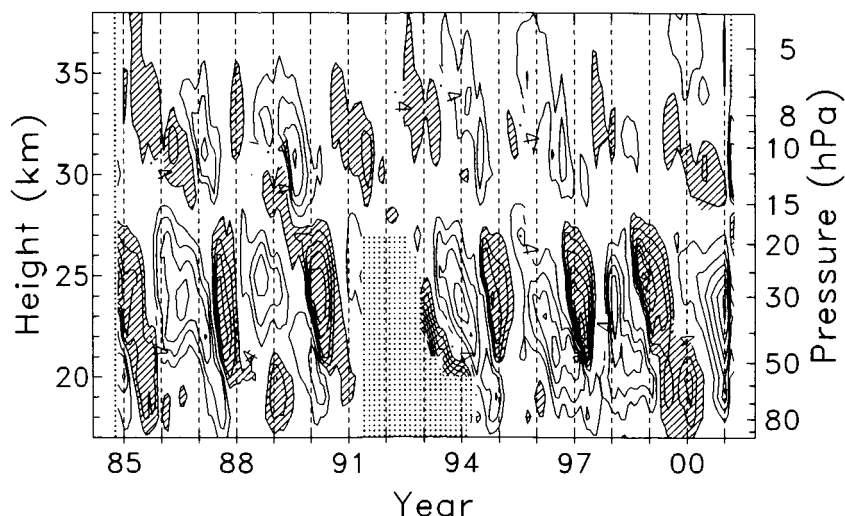


Figure 9. Contour plot of ozone anomalies for 2°N – 2°S from SAGE II data, calculated with the methodology of *Randel and Wu* [1996]. Data gaps were filled by interpolation (including the last 6 months of 2000), and a 1:2:1 smoothing was applied. Contour intervals are ± 0.4 DU/km, positive contours are shaded, and the zero contour is omitted.

[25] A contour plot of the monthly anomalies for Ascension (not shown) indicates that the amplitude of the QBO signal is +10% in early 1998 at 30 hPa, about half of that for the equatorial stations. However, the amplitude of the feature at 60–70 hPa is about the same as that for the equatorial stations. This is apparent also in Figure 7.

[26] The monthly ozone and temperature anomalies in the tropical lower stratosphere were likely influenced by the major El Niño–Southern Oscillation (ENSO) warm event that occurred in 1997–1998. Pacific sea surface temperatures were anomalously warm from mid-1997 to northern spring 1998, with the largest anomaly in late 1998 (<http://ncep.noaa.gov>). *Reid et al.* [1989] have shown that during the ENSO warm phase, stratospheric temperatures in the equatorial region are cooler than usual from about 100 to 40 hPa; the cooling in the stratosphere lags the warming in the troposphere by about 3 months, and takes place primarily in northern winter [Reid, 1994]. In late 1997 and early 1998, the descending westerly phase of the QBO would normally have produced a positive anomaly in ozone and temperature below 40 hPa, but Figures 8 and 9 show primarily a negative anomaly in ozone (and in temperature, not shown) owing to the effect of ENSO on the lower stratosphere. A parallel situation existed in the winters of 1987/88 and 1994/95 with regard to both warm ENSO events (weaker than in 1997/98) and the equatorial winds, and the SAGE II data show that there is a negative ozone anomaly below 20 km at these times also; note that the positive ozone anomaly does not descend past 20 km in each case. Similarly it is likely that the cold ENSO events of the winters of 1985/86, 1988/89, and 1999/2000 reinforce the positive ozone anomalies below 20 km in those seasons (Figure 9).

[27] The dramatic change in the shape of the ozone profile in 1998 seen in Figure 4 for Nairobi is found also at San Cristobal, and similar changes are found for both

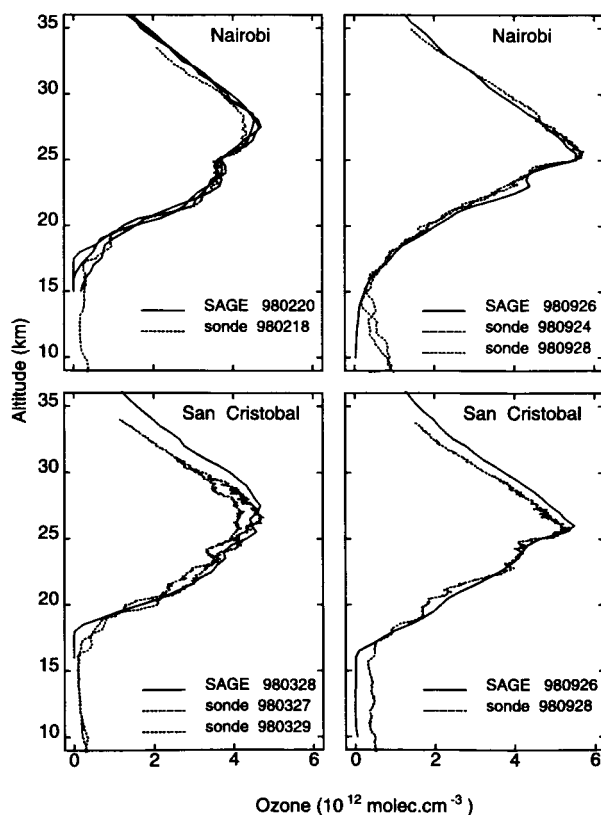


Figure 10. Comparison of ozone profiles measured by SAGE II (solid) and by ozonesondes (dashed) over Nairobi (upper) and San Cristobal (lower). The SAGE II profiles were obtained within 2° of latitude, and 35° of longitude of the sondes. Dates are given in the format year, month, day.

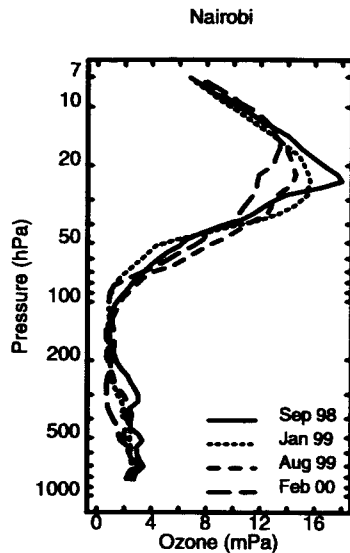


Figure 11. Monthly mean profiles for Nairobi for September, 1998, January, 1999, August, 1999, and February, 2000.

stations in 2001, at a similar phase of the QBO. The change in shape is less severe for Ascension at the ozone maximum (not shown). Figure 11 shows how the shape of the Nairobi profile changes from the time of maximum ozone in September 1998 to the time of minimum ozone in February 2000. The altitude of the maximum increases as its value

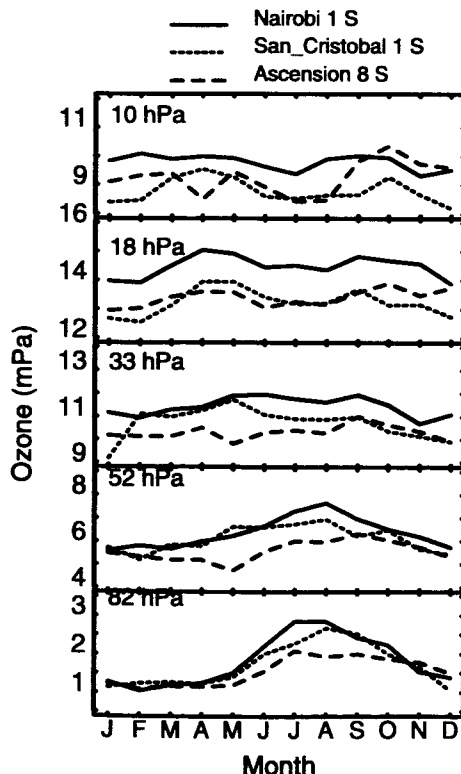


Figure 12. Seasonal cycle of ozone for Nairobi, San Cristobal, and Ascension.

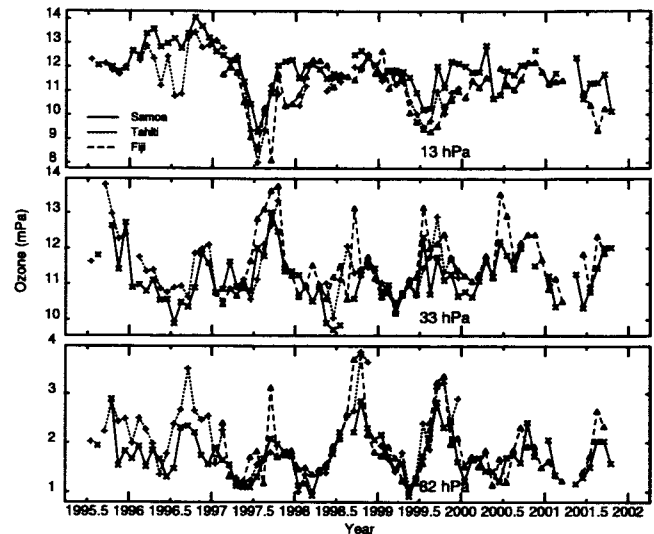


Figure 13. Time series of monthly mean values for ozone in mPa over Samoa (solid), Tahiti (dotted) and Fiji (dashed).

declines. The difference in the profile in the lower stratosphere between March and September/October reflects primarily the seasonal cycle rather than the QBO. The mean seasonal cycle for these stations is shown in Figure 12. Ozone concentrations are lowest from December to April and highest from July to September from the tropopause to about 50 hPa; there is then a transition to a semiannual cycle which is apparent by 20 hPa. This behavior is similar to the seasonal cycle in temperature, which also shows a transition from an annual cycle to a semi-annual cycle near 35 hPa [e.g., Reid, 1994].

3.2. Ozone at 14° to 20°S

[28] We examined the data from Samoa, Tahiti and Fiji for evidence of a QBO signal. The data from these locations encompass two QBO cycles, with observations at Samoa and Tahiti starting in late 1995 and Fiji in early 1997; observations at Tahiti ended in 1999. Easterly equatorial winds descend through 20 hPa in August, 1995, with the easterly phase lasting 15 months; equatorial winds are westerly at this level from November, 1996, until October, 1997. Monthly mean values of ozone are similar at the three stations, as shown in Figure 13. The seasonal cycle in ozone is readily apparent from the tropopause to about 35 hPa. QBO signatures are evident in the contour plots of the smoothed anomalies for Samoa and Fiji, as shown in Figure 14. There is a QBO signature from the top of the soundings at 7 hPa down to about 20 hPa with an amplitude of about $\pm 10\%$ that is seasonally synchronized, with maxima and minima in austral winter/spring. A weaker QBO-like signature is apparent from 25 to 50 hPa, with an amplitude of ± 5 – 10% at Fiji and a somewhat smaller amplitude at Samoa; it is out of phase with the signal above it. There is a third set of anomalies from 50 hPa to 90 hPa with an amplitude of ± 15 – 30% , which are usually out of phase with those from 25 to 50 hPa; these are not necessarily related to the QBO.

[29] The effect of the QBO on the ozone profile over Samoa is illustrated in Figure 15 which compares profiles

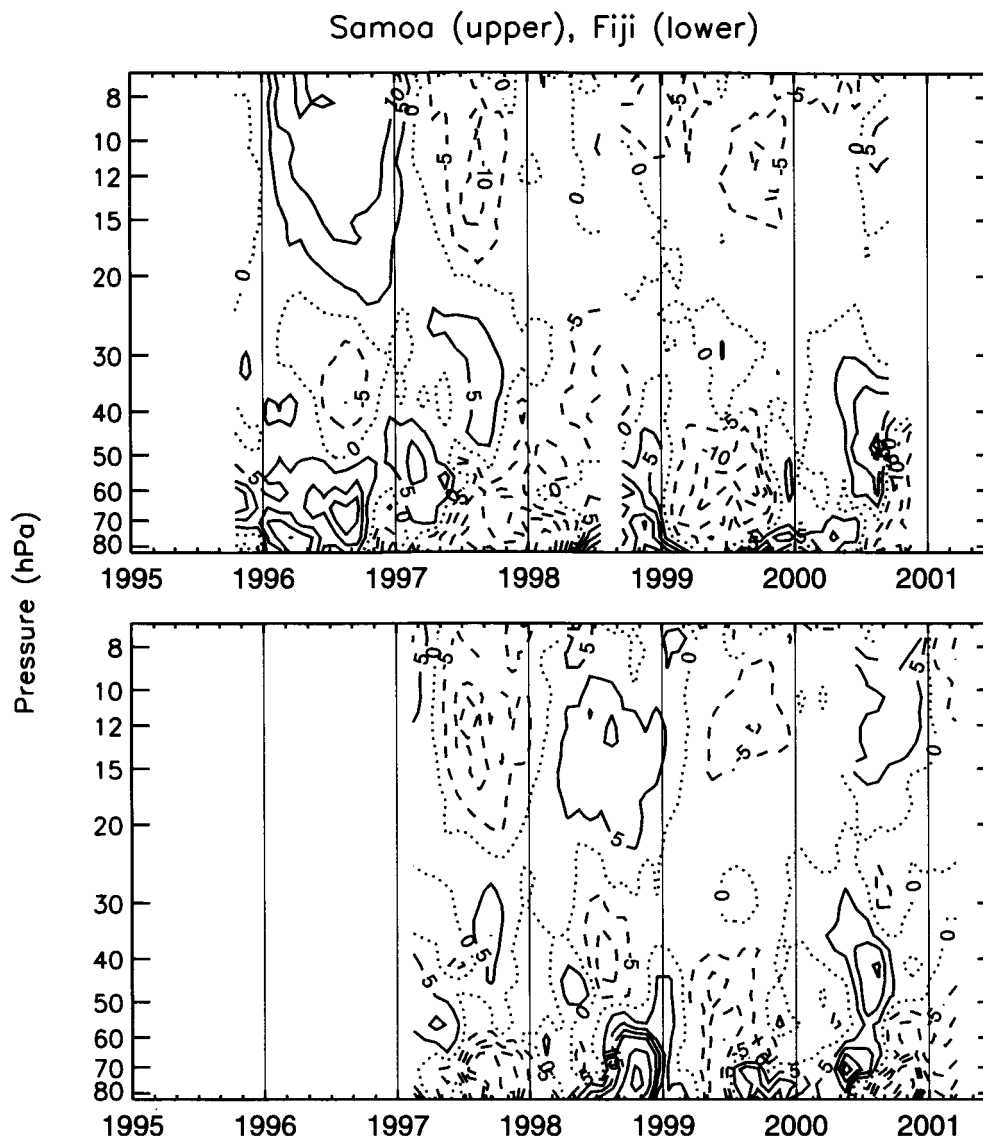


Figure 14. Contour plots of smoothed monthly ozone anomalies for Samoa (upper panel) and Fiji (lower panel) in percent. The anomalies are 3-month running means, contoured by 0, \pm (5, 10, 15, 20, 30, 40%). Positive contours are solid, the zero contour is dotted, and negative contours are dashed.

for July, 1996, and August, 1997. Between these two times, the westerly shear zone over the equator descended from 10 hPa to below 50 hPa; this causes upwelling in the subtropics, and hence the lower ozone values below 50 hPa. Meanwhile a new easterly shear zone on the equator crossing 10 hPa in mid-1997 causes downwelling in the subtropics, explaining the downward motion of the ozone maximum. The ozone maximum descends from 18 hPa to 26 hPa, but its concentration does not change, in contrast to the situation over the equator, where the ozone maximum descends and its value increases significantly (Figure 4).

[30] The QBO anomalies in SAGE data are shown in Figure 16 for 18° – 22° S in units of DU/km. There is good qualitative agreement between the SAGE contour map and those for Samoa and Fiji. The SAGE anomalies for 20° S are ± 6 – 12% at 22.5 km, slightly smaller than those derived from the sondes. The SAGE anomalies also show

a three-cell structure, and in many years the signs of the anomalies alternate, particularly in the 1990s. However, there are years in the 1980s where the upper and middle anomalies are of the same sign. The contributions of the three altitude regions to the column anomaly are quantified in section 4.

3.3. Ozone at 20° N

[31] Ozonesonde measurements have been made regularly at Hilo, Hawaii, since 1985, with a gap of a few months in early 1991 [Hofmann *et al.*, 1993]. Monthly mean time series are shown for 13 and 33 hPa in Figure 17. There is a clear seasonal cycle at these levels, in contrast to the data from similar latitudes in the southern hemisphere, where the seasonal cycle is less apparent (Figure 13). A comparison of the seasonal cycles for Hilo and Samoa presented in Figure 18 shows that the amplitude is larger at Hilo, except near 50 and 10 hPa. There is little evidence

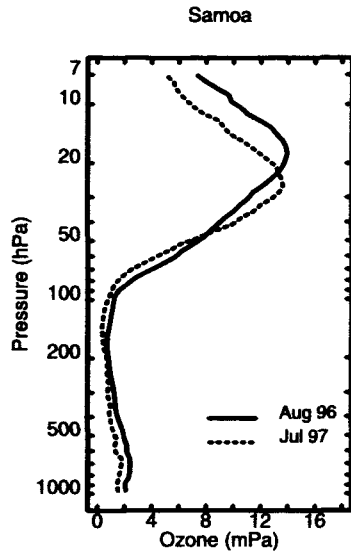


Figure 15. Comparison of monthly mean profiles for August, 1996, and July, 1997, over Samoa, comparing two phases of the QBO signal evident in Figure 14.

of a semi-annual oscillation at 10 hPa at either station, although it is apparent at 10 hPa over the equator, as shown by the data from San Cristobal.

[32] A contour plot of smoothed anomalies for Hilo is shown in Figure 19. There is a QBO signature from above 7 hPa to about 15 hPa with an amplitude of ± 5 –15% that is seasonally synchronized, with maxima and minima in late northern winter. A second QBO signature is located from 25 to 55 hPa, with an amplitude of -10 to $+10$ –20%, which is often in phase with the signature above it. Below 55 hPa, there is interannual variability, but much of this appears to be associated with temperature anomalies in the lower stratosphere related to ENSO as discussed in section 5.

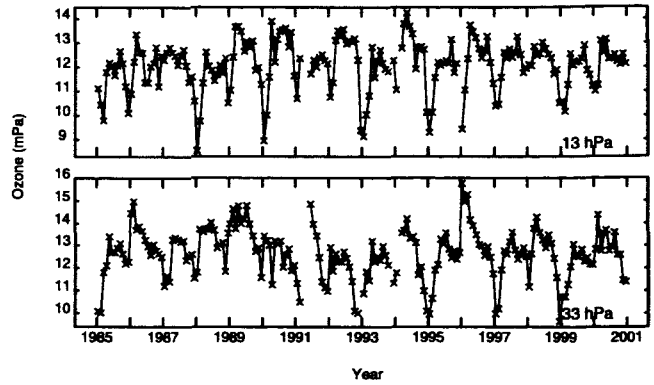


Figure 17. Time series of monthly mean values for ozone in mPa over Hilo, Hawaii.

There are negative temperature anomalies below 60 hPa (not shown) in warm ENSO winters (1986–87, 1991–1992, 1994–1995, and 1997–1998), and most of these periods show negative ozone anomalies. There are positive temperature anomalies during major cold ENSO winters (1988–89 and 1999–2000), and these periods show positive ozone anomalies.

[33] A contour plot of the smoothed SAGE ozone anomalies for 18° – 22° N is shown in Figure 20 in DU/km. There is reasonable qualitative agreement between the SAGE contour map and that for Hilo. The amplitudes of the SAGE anomalies for 20° N are ± 6 –12% at 22.5 km, slightly smaller than those derived from the sondes. The SAGE data often show a three-cell structure, and the upper and middle anomalies are generally of the same sign, especially in the 1990s, as shown quantitatively in section 4.

[34] *Leblanc and McDermid* [2001] recently presented an analysis of QBO signatures in ozone and temperature at Mauna Loa, Hawaii, based on lidar data from 1994 to mid-2000 for 20–55 km (55–0.5 hPa). They find similar results

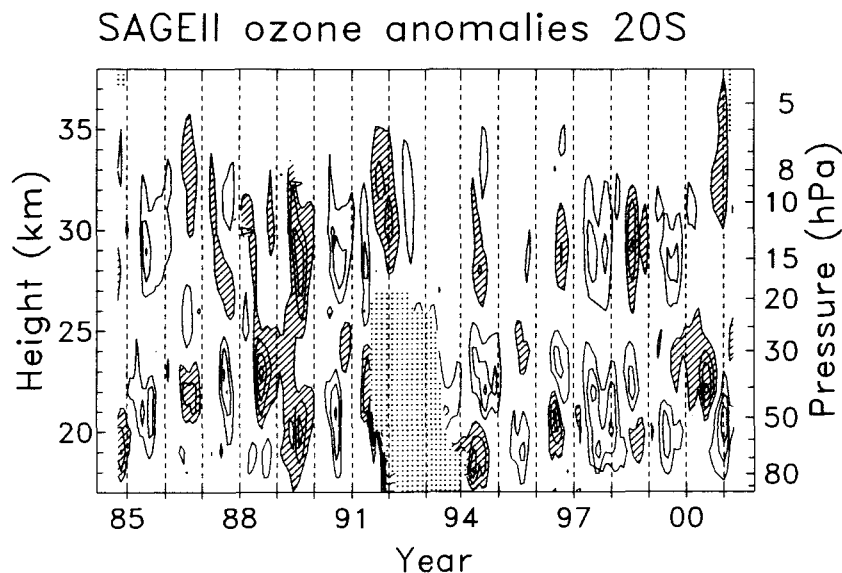


Figure 16. Contour plot of ozone anomalies for 18° – 22° S from SAGE II data, calculated with the methodology of *Randel and Wu* [1996]. Contour intervals are ± 0.4 DU/km, positive contours are shaded, and the zero contour is omitted. See Figure 9 for other details.

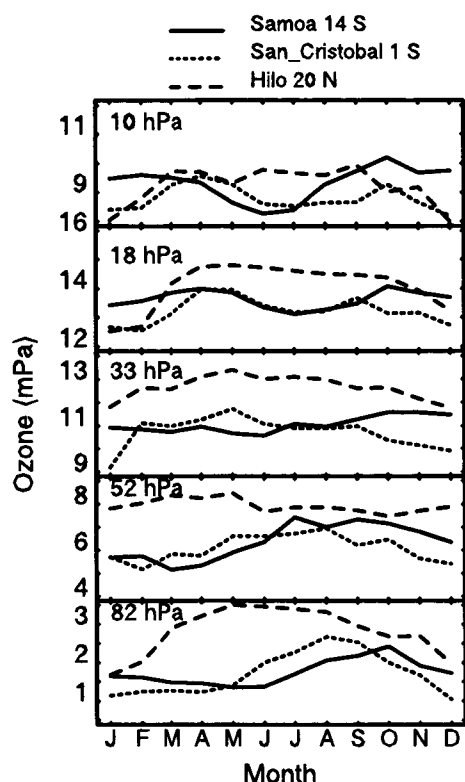


Figure 18. Seasonal cycle of ozone for Hilo (20°N), San Cristobal (1°S), and Samoa (14°S).

for ozone to those shown in Figure 19 with one exception. In 1997 the lidar data indicate a positive ozone anomaly at the start of the year from 55 to 20 hPa and a negative anomaly from March until early 1998, while the sonde data show a negative anomaly in most of 1997, until the end of the year, when a strong positive anomaly develops at 50 hPa. The SAGE data also show a negative anomaly in the same region (21–26 km) for the first half of 1997. The measurement frequency of the lidar data is greater than that of the weekly sonde measurements, so the former should be more representative for Hawaii, while the SAGE data represent the zonal mean. Leblanc and McDermid argue that the negative ozone anomalies they see in 1997 and early 1998 below 25 hPa are in part a manifestation of the strong ENSO event. The positive anomaly at 50 hPa in late 1997 in the sonde data is caused by a layer of high ozone in one profile in December whose influence is exaggerated by the 3-month smoothing in Figure 19. Ozone is highly variable in the lower stratosphere in winter over Hawaii as discussed in section 5

4. Analysis of the QBO in Column Ozone Derived From TOMS/SBUV, SAGE II, and Sondes

[35] There is usually good agreement among column ozone anomalies derived from the three data sets considered here, as shown in Figure 21. This comparison uses the SAGE and TOMS/SBUV data averaged over the same 4° latitude bands. The sonde record is noisier because only 1–4 measurements per month were included; 25–35% of profiles were omitted because they did not reach 8 hPa.

Comparison of TOMS overpass data with zonal mean values indicates that some of the differences between sonde and TOMS for 20°N and 20°S are caused by longitudinal variations in column ozone. The largest discrepancy between the SAGE and TOMS/SBUV columns in Figure 21 occurs in December 1993 and January 1994, when there is an unusually large ozone anomaly below 20 km (see Figure 20). We attribute this discrepancy to ozone data that were not removed by the filter for high aerosol loading after Pinatubo, and disregarded these SAGE data in subsequent analyses.

[36] The monthly anomalies for column ozone from 1985 to 2000 are shown in Figure 22 for 30°N to 30°S in percent. We did not remove the solar cycle from the column data (as is generally done) for the sake of consistency, because we will make comparisons below with the monthly anomalies in the profile data. The anomalies at the equator usually exceed $\pm 4\%$, while those in the subtropics are not always as large as this. The subtropical anomalies are seasonally synchronized in local winter/spring, and are usually out of phase with those over the equator, as known from earlier studies [Bowman, 1989; Hamilton, 1989; Lait *et al.*, 1989].

[37] The monthly anomalies for ozone at 22.5 km derived from SAGE data are shown as a time-latitude plot in Figure 23. This cross section is at the maximum of the lower band of equatorial anomalies. As for the column, the anomalies at 20°N and 20°S are usually out of phase with those over the equator, and prefer local winter/spring. However, the ozone anomalies in the lower stratosphere at 20°S lag those at the equator by a few months during the easterly phases of the QBO from 1994 to 1998. The ozone anomalies generally extend from the subtropics into the midlatitudes in the northern hemisphere, but this behavior is seen in the southern hemisphere only in the 1980s and in 1997. Earlier analyses of the QBO in column ozone have also shown that there are periods when the subtropical signature is stronger in one hemisphere than the other, and sometimes missing in one particular hemisphere [e.g., Gray and Dunkerton, 1990; Gray and Ruth, 1993].

[38] The relationship between the subtropical and equatorial QBO anomalies in column ozone depends on the timing of the equatorial winds with respect to the annual cycle [Bowman, 1989; Hamilton, 1989; Lait *et al.*, 1989]. The QBO induces significant modulation of the mean meridional circulation, which is very asymmetric during the solstices [Jones *et al.*, 1998; Kinnery, 1999]. The induced circulation is stronger in the winter hemisphere. The formation of a strong winter subtropical anomaly in ozone requires first that there is strong vertical shear in the lower stratosphere (below about 20 hPa) at the equator to induce a QBO circulation, and second that there is strong background horizontal advection of zonal momentum, in order to strengthen the induced QBO circulation in the winter hemisphere [Baldwin *et al.*, 2001]; then these conditions must persist for one to two months so that ozone can respond to the induced circulation. Thus the strong vertical shear must be in late fall and/or early winter for there to be a strong winter subtropical anomaly.

[39] Here we present a quantitative analysis of the contributions of the ozone anomalies at different altitudes to the column anomaly. Empirically, we find that when the subtropical column anomaly is strong, the tropical wind shear is

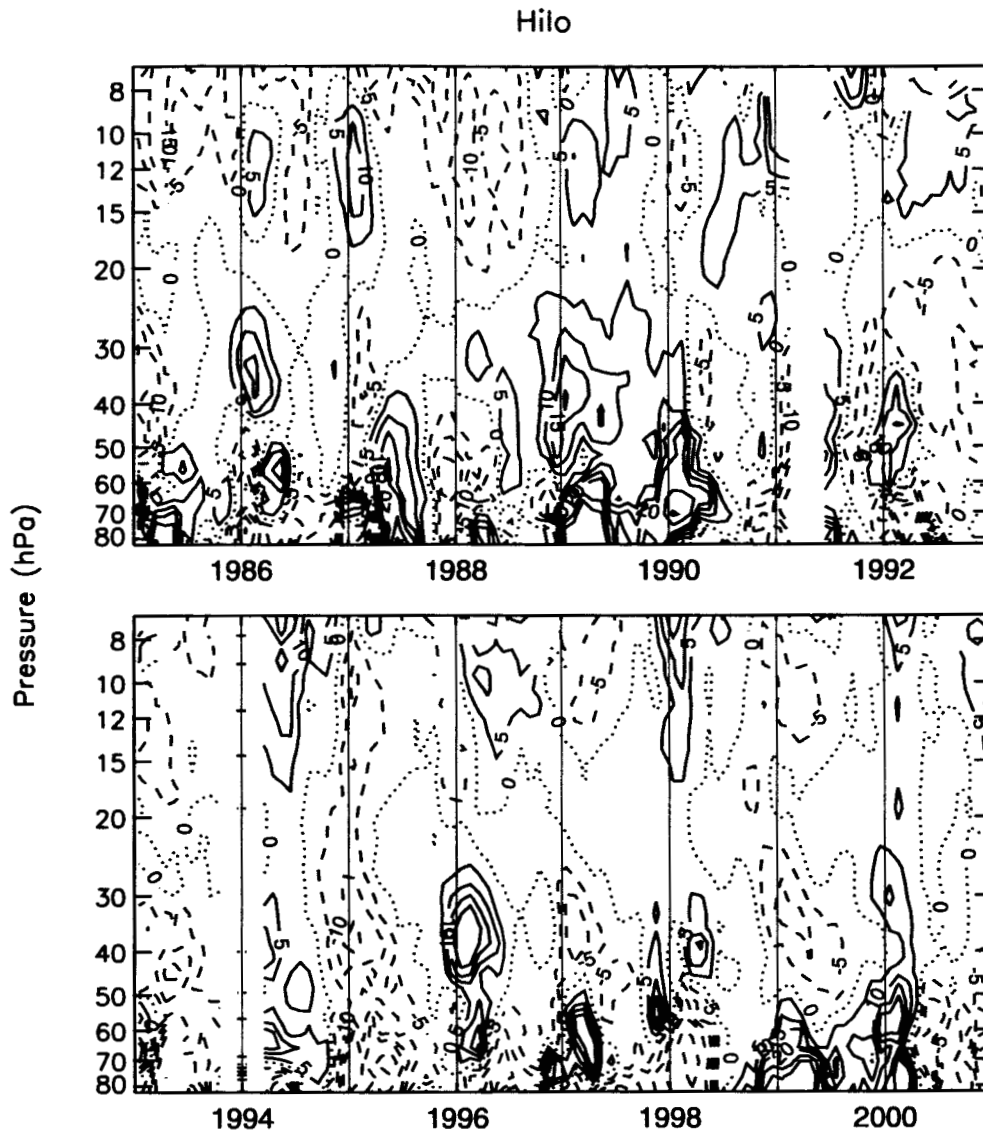


Figure 19. Contour plot of monthly anomalies for Hilo, Hawaii, for 1985 to 2000, in percent. The anomalies are 3-month running means, contoured by 0, \pm (5, 10, 15, 20, 30, 40). Positive contours are solid, the zero contour is dotted, and negative contours are dashed.

strong in early winter below 20 hPa, and the upper and middle ozone anomalies reinforce each other. Conversely, when the column anomaly is weak, the tropical wind shear is often strongest above 20 hPa, and the upper and middle ozone anomalies often cancel one another, or one of them is absent.

[40] The contribution of the ozone anomalies in different altitude regions to the column anomaly are shown in Figures 24a through 26b. The altitude regions were selected based on the three-cell structure evident in Figures 16, 19, and 20. The results are averages for December–March at 20°N and for June–September for 20°S. These months were selected as some of the winter/spring anomalies are rather narrow, but results are similar if extended for another month. We required that SAGE data were available for 3 of the 4 months to be included in the analysis. Results are shown separately for strong (>5 DU) and weak (<5 DU) column anomalies, as defined by the TOMS/SBUV record

(5 DU is $\sim 2\%$ of the column). Figures 24a to 26a, using SAGE and sonde data, show that the strong QBO signals in column ozone occur when the ozone anomalies above 27 km (20 hPa) and from 21 to 27 km (50 to 20 hPa) are of the same sign and reinforce one another; for the few exceptions to this pattern, the SAGE or sonde column anomaly does not agree very well with the TOMS/SBUV anomaly. Figures 24b to 26b show that the weak signals in column ozone typically occur when the ozone anomalies above 27 km and from 21 to 27 km either cancel one another or one of them is absent or very small. The column anomalies in the lowest part of the stratosphere, below 20 km, sometimes make a significant contribution to the column anomaly.

[41] The TOMS/SBUV record shows that strong column anomalies were more common in the northern subtropics between 1985 and 2000, 10 of 16 cases, compared to the southern subtropics, 7 of 16 cases. (These cases are not all illustrated in Figures 24a, 24b, 26a, and 26b, as SAGE data

SAGEII ozone anomalies 20N

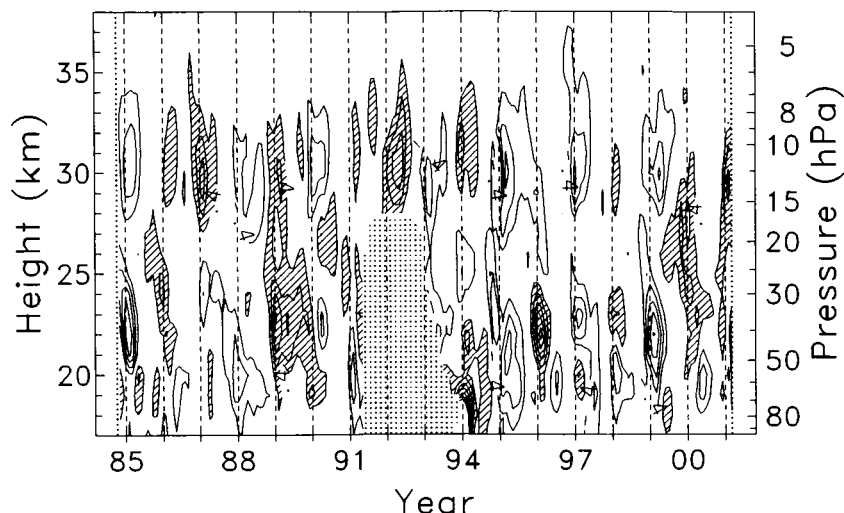


Figure 20. Contour plot of ozone anomalies for 18° – 22° N from SAGE II data, calculated with the methodology of *Randel and Wu* [1996]. Contour intervals are ± 0.4 DU/km, positive contours are shaded, and the zero contour is omitted. See Figure 9 for other details.

are missing from mid-1991 to 1993.) Between 1985 and 1991, there were 4 strong and 3 weak column anomalies at 20° N, while there were 4 strong and 2 weak column anomalies at 20° S. In the 1990s there was a bias towards strong column anomalies at 20° N, 5 of 7 cases for 1993/94 to 1999/2000. In contrast, at 20° S, column anomalies were

strong in only 1 of 6 cases for 1994 to 1999. Column data are lacking for 20° S for 1993, and those in 1992 are perturbed by the eruption of Pinatubo.

[42] We consider now the influence of the wind shear on the strength of the column anomalies. The wind shear at 35 hPa is shown in Figure 27. This level was selected to

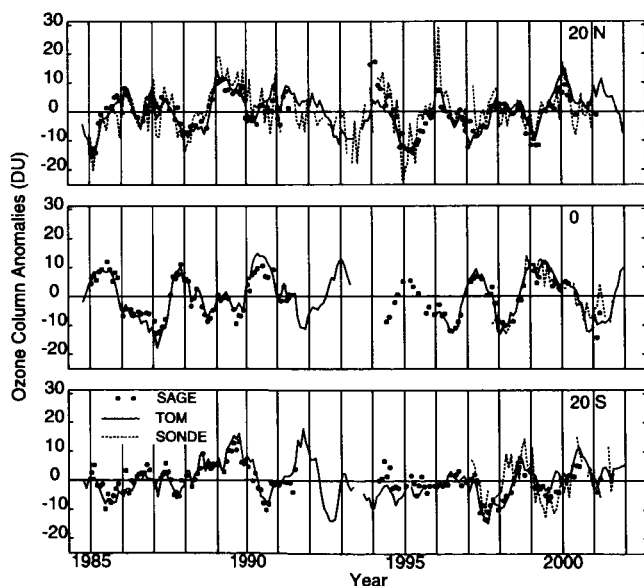


Figure 21. Comparison of monthly anomalies in column ozone from TOMS/SBUV (solid line), SAGE (filled circles), and sondes (dotted line). The TOMS and SAGE anomalies are zonal means for a 4° latitude band centered at $\pm 20^{\circ}$ and 0° ; the SAGE anomalies are integrated columns from 16.5 to 35.5 km; the sonde data are from Hilo (20° N), Nairobi (1° S), and Fiji (18° S), integrated from 100 to 8 hPa (16.5 to 32.5 km). None of the data sets have been interpolated or smoothed.

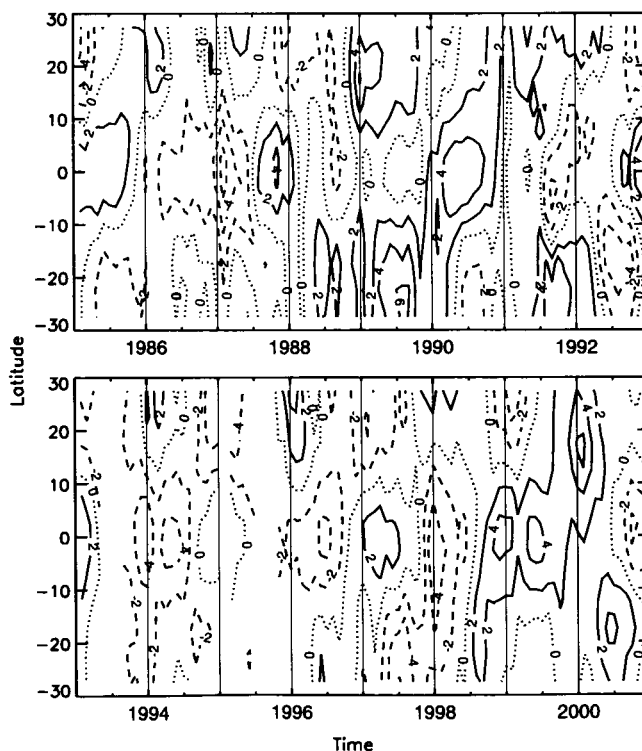


Figure 22. Contour plot of monthly anomalies in column ozone from TOMS/SBUV. Contours are 0, ± 2 , and ± 4 percent. Positive contours are solid, the zero contour is dotted, and negative contours are dashed.

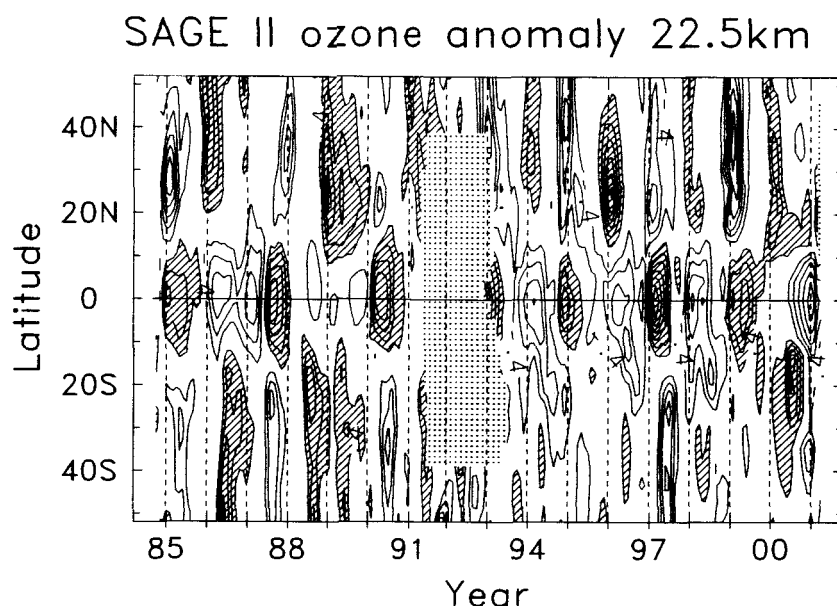


Figure 23. Contour plot of ozone anomalies at 22.5 km from SAGE II data, calculated with the methodology of *Randel and Wu* [1996]. Contour intervals are ± 0.4 DU/km, positive contours are shaded, and the zero contour is omitted. See Figure 9 for details.

represent the lower stratosphere as it is in the middle of the lower equatorial ozone anomaly. As discussed above, there should be strong vertical shear in late fall and/or early winter for there to be a strong subtropical anomaly in winter/spring. For the northern subtropics we define strong shear to be values higher than 80% of the maximum (or minimum)

shear in October to January that persist for at least 2 months; we used the months of April to July in considering the shear conditions relevant to 20°S . With this definition, the wind shear is strong at 35 hPa during northern late fall and early winter for the eight periods marked “MAX” and “MIN” (for positive and negative shear) in Figures 24a through 26b.

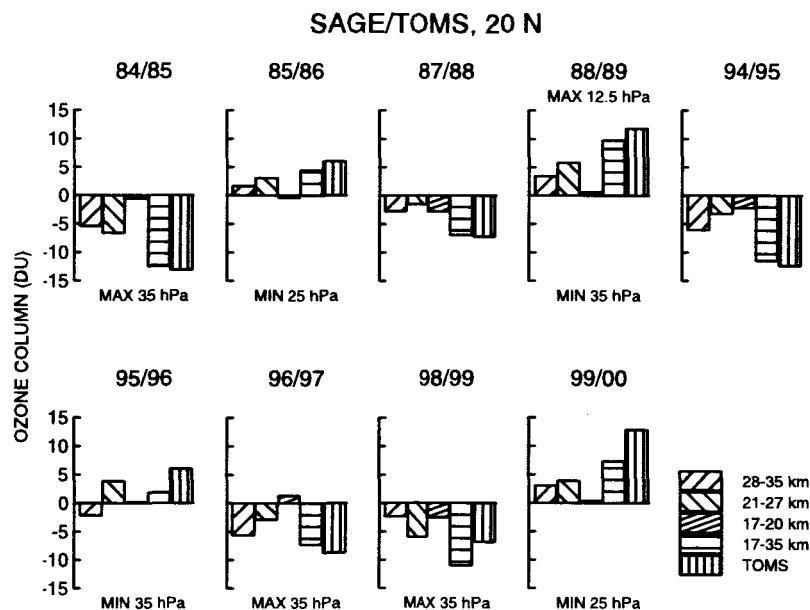


Figure 24a. The contribution of different altitudes to the column ozone anomaly, derived from SAGE and TOMS/SBUV data for 18° – 22°N . Results are shown for TOMS/SBUV larger than 5 DU. Each panel gives the mean for December to March for the years indicated. From left to right, the bars are the ozone column anomaly for: 28–35 km, 21–27 km, 17–20 km, 17–35 km, all from SAGE; and the total column anomaly from TOMS/SBUV. The labels “MAX at 35 hPa” etc. show that there was strong positive shear at that pressure level in the preceding late fall or in early winter, as discussed in the text; the labels with “MIN” refer to strong negative shear.

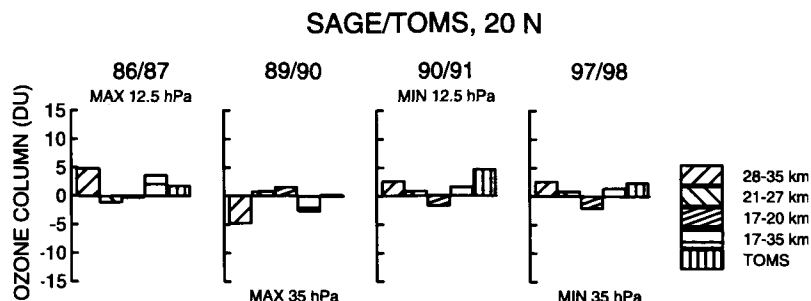


Figure 24b. The contribution of different altitudes to the column ozone anomaly, derived from SAGE and TOMS/SBUV data. Results are shown for TOMS/SBUV smaller than 5 DU. See Figure 24a for other details.

For 20°N, there is a high column signal in December to March for 5 of the 8 periods with strong shear in late fall/early winter; this increases to 7 of 10 cases if we include 1985/86 and 1999/2000 when there was strong shear at 25 hPa that stalled above 35 hPa. Of the three cases without a high column signal, one is 1997–1998, when the positive phase of the QBO in the lower stratosphere is lacking at 20°N because of the cool stratospheric temperatures associated with the strong ENSO warm phase [Leblanc and McDermid, 2001]; another, 1989/90, is the only one of the 8 cases when the strong shear at 35 hPa started as late as

January. In the southern subtropics, there is strong shear in late fall/early winter for only 5 years, 1986, 1989, 1991, 1992, and 2000, for 3 of which SAGE data are lacking in June–September (section 2); if we choose a higher altitude for the shear, 25 hPa, then 1988 and 1993 would also fall in this category. There is a strong column signal at 20°S in 5 of these years, with 1986 as the only exception (TOMS/SBUV data are lacking for mid-1993). Clearly, strong shear in late fall/early winter is usually associated with a strong signal in subtropical column ozone in winter/spring, but is the converse true? We find that about half the cases with a strong

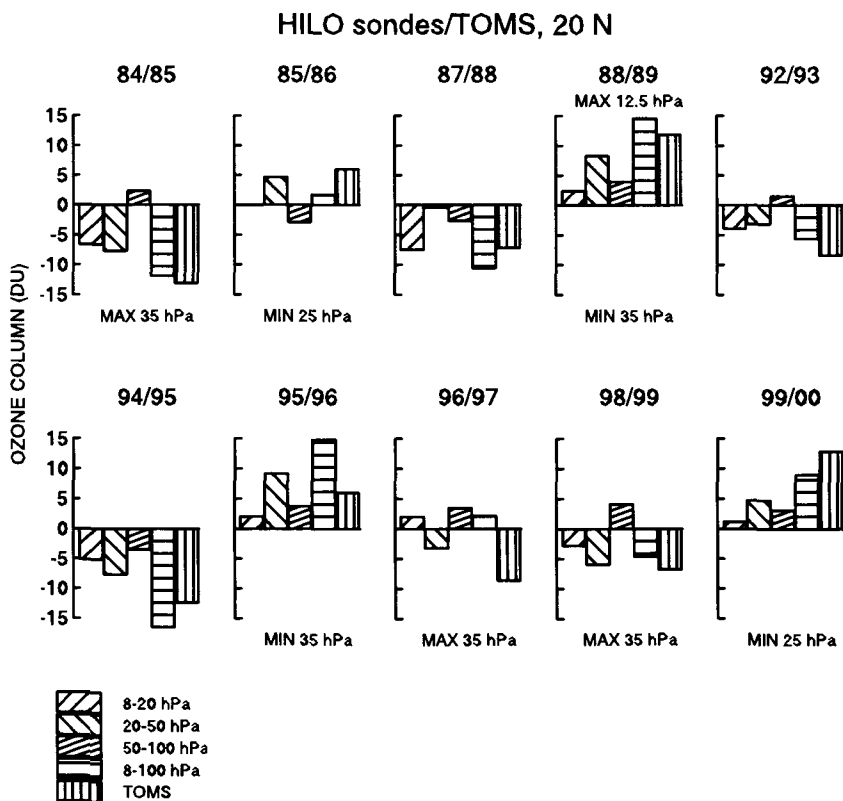


Figure 25a. The contribution of different altitudes to the column ozone anomaly, derived from sonde data for Hilo (20°N) and TOMS/SBUV data (18°–22°N). Results are shown for TOMS/SBUV larger than 5 DU. Each panel gives the mean for December to March for the years indicated. From left to right, the bars are the ozone column anomaly for: 8–20 hPa, 20–50 hPa, 50–100 hPa, 8–100 hPa, and the total column anomaly from TOMS/SBUV. See Figure 24a for other details.

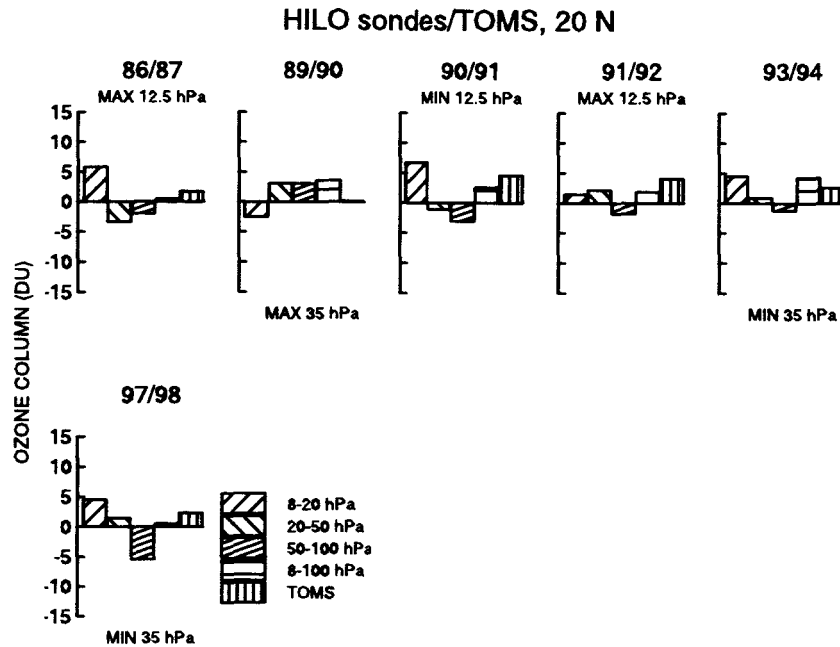


Figure 25b. The contribution of different altitudes to the column ozone anomaly, derived from sonde data for Hilo (20°N) and TOMS/SBUV data (18°–22°N). Results are shown for TOMS/SBUV smaller than 5 DU. See Figure 25a for other details.

signal in column ozone are associated with strong shear at 35 hPa in the preceding late fall/early winter cases, 5 of 10 at 20°N, and 3 of 7 at 20°S. If we include the wind shear at 25 hPa also as a reference, this increases to 7 of 10 cases at 20°N and 5 of 7 at 20°S. However, for the weak signals in column ozone, only 1 of 7 at 20°S has strong shear in the preceding late fall/early winter, but 3 of 6 at 20°N.

[43] We consider now the influence of the wind shear in the middle stratosphere on the subtropical QBO. The wind shear for 12.5 hPa is shown in Figure 27; this level is the highest altitude for which the wind shear could be calcu-

lated for 1985–2001. Figures 24b to 26b show that when there is a weak QBO signal in column ozone, there is often strong shear in the middle stratosphere, 3 of 6 cases at 20°N and 5 of 7 cases at 20°S. (We did not require that the strong shear persisted at 80% of its maximum for 2 months for the narrow shear zones in 1994 and 1995). The ozone anomaly is positive for 8–20 hPa (above 27 km) for westerly equatorial shear, and negative for easterly shear, as expected from the influence of dynamically induced variations in NO_y . The only exception is 1990/91 at 20°N, when the upper anomaly is positive in a region of easterly shear. We

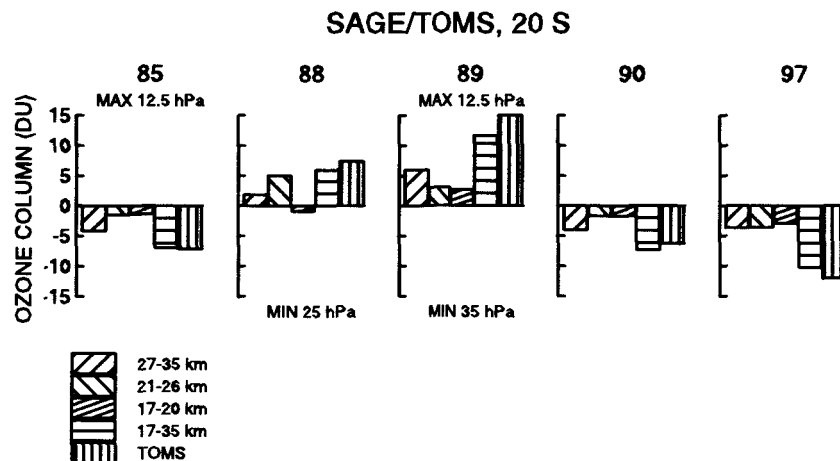


Figure 26a. The contribution of different altitudes to the column ozone anomaly, derived from SAGE and TOMS/SBUV data for 18°–22°S. Results are shown for TOMS/SBUV larger than 5 DU. Each panel gives the mean for June to September for the year indicated. From left to right, the bars are the ozone column anomaly for: 27–35 km, 21–26 km, 17–20 km, and 17–35 km, all from SAGE; and the total column anomaly from TOMS/SBUV. See Figure 24a for other details.

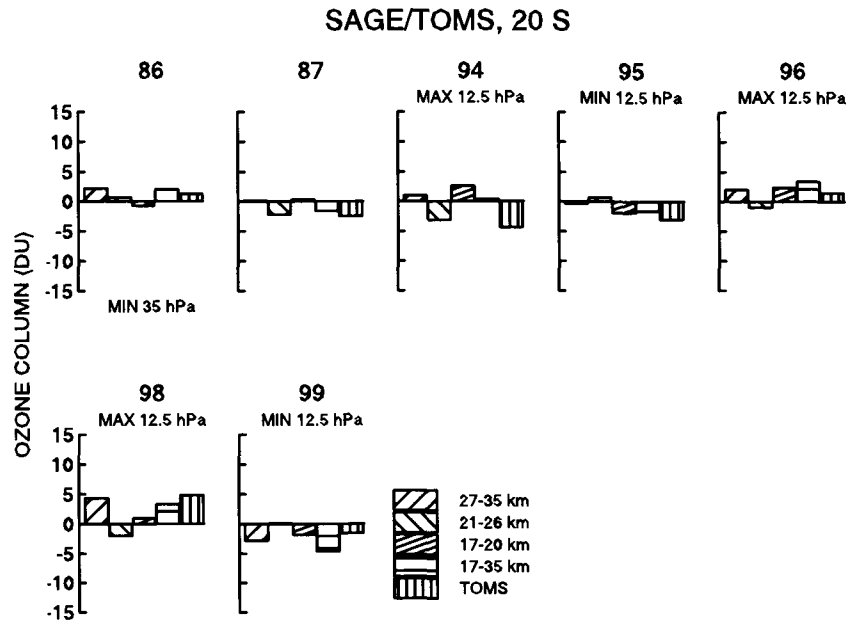


Figure 26b. The contribution of different altitudes to the column ozone anomaly, derived from SAGE and TOMS/SBUV data for 18°–22°S. Results are shown for TOMS/SBUV smaller than 5 DU. See Figure 26a for other details.

find also that the anomaly below 27 km is either of opposite sign, or not present, except for 1988/89 at 20°N and 1989 at 20°S when strong shear was also present in the lower stratosphere. The last two cases with strong shear in both the middle and lower stratosphere in the appropriate season are two of the strongest column signals in the record.

5. Contributions of the Seasonal Cycle and the QBO to the Variance in Ozone

[44] We applied linear regression models to evaluate the contributions of the seasonal cycle and the QBO to the ozone time series for Nairobi, Samoa, and Hilo. Admittedly the length of record is rather short for Nairobi, as it encompasses only two QBO cycle, but the results are interesting as a point of comparison with the subtropics. For the equator, the model for the ozone time series at a given pressure, $O_3(t)$, is

$$O_3(t) = \sum_{i=1}^{12} \mu_i I_{i,t} + \gamma Z_{t-k} + E_t \quad (1)$$

where μ_i is the mean ozone amount in month i , $i = 1, \dots, 12$; $I_{i,t}$ is an indicator series for month i of the year which is equal to 1 if t corresponds to month i of the year and zero otherwise; Z_{t-k} is the Singapore zonal wind at the same level lagged by k months, with γ the associated coefficient; and E_t is the residual error. The winds were interpolated to the same pressure levels as ozone for use in (1). We ran the model for a range of lags from -15 to 6 months. A negative lag indicates that the winds precede ozone. We also fit the data with the seasonal cycle and with the QBO term separately.

[45] Figure 28 shows r^2 for the model fits to the ozone time series for Nairobi. Results are shown for the lag that gives the best fit to the data at each pressure, and for the

model with the QBO term alone and the seasonal term alone. Figure 29 shows the model fit for selected pressure levels. The full model explains more than 75% of the variance of the monthly means from 15 to 95 hPa, and as much as 85% from 25 to 35 hPa. The QBO term dominates the variance from 20 hPa to about 50 hPa, and the seasonal cycle dominates the variance from 55 to 95 hPa. The two terms are similar in magnitude from 10 to 18 hPa. The fit to the QBO term is statistically significant at all levels ($p < 0.05$). From 20 to 70 hPa, the best fit is for a lag of 3 to 5 months, that is the phase of the ozone QBO precedes that of the winds (see Figure 8); the ozone QBO lags the winds by 8 months at 18 hPa, with the lag progressively decreasing with pressure to 1 month by 11 hPa. Hasebe [1994] found similar results for lagged correlations between SAGE II ozone anomalies and the zonal wind. The best fit lag changes sign at the top of the lower anomalies where ozone acts as a dynamical tracer.

[46] We ran the model for Nairobi with wind shear instead of wind for Z_{t-k} in equation (1); this gave a slightly

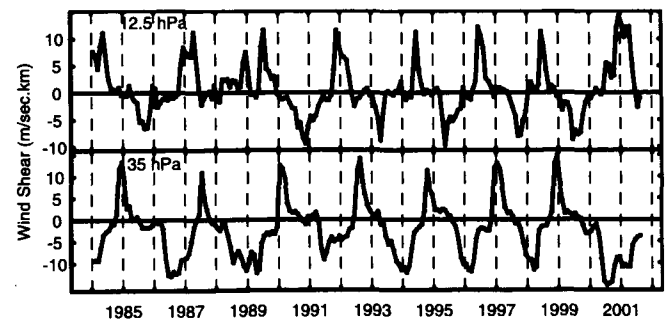


Figure 27. Wind shear at 12.5 hPa and 35 hPa calculated from the monthly mean zonal wind component at Singapore.

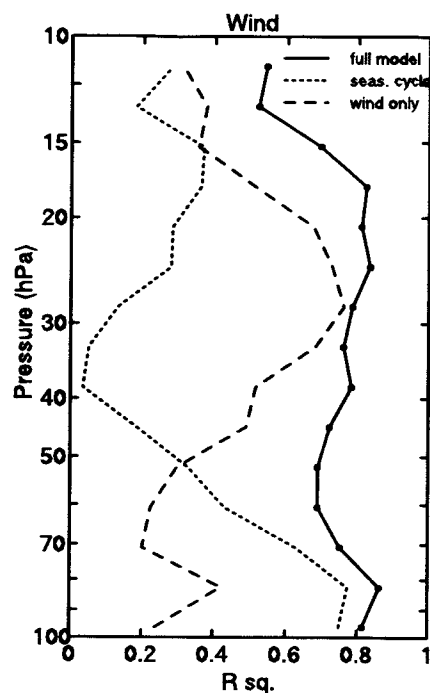


Figure 28. Vertical profile of r^2 for the regression model given by equation (1) for Nairobi (solid line). The dashed lines shows results using only the wind in the model fit, and the dotted line shows results using only the seasonal cycle in the model fit.

better fit than the model with winds only near 30 hPa and near 10 hPa (not shown). The best fit for this model from 20 to 60 hPa was with the wind shear preceding the ozone by a month or synchronous with it, consistent with the observa-

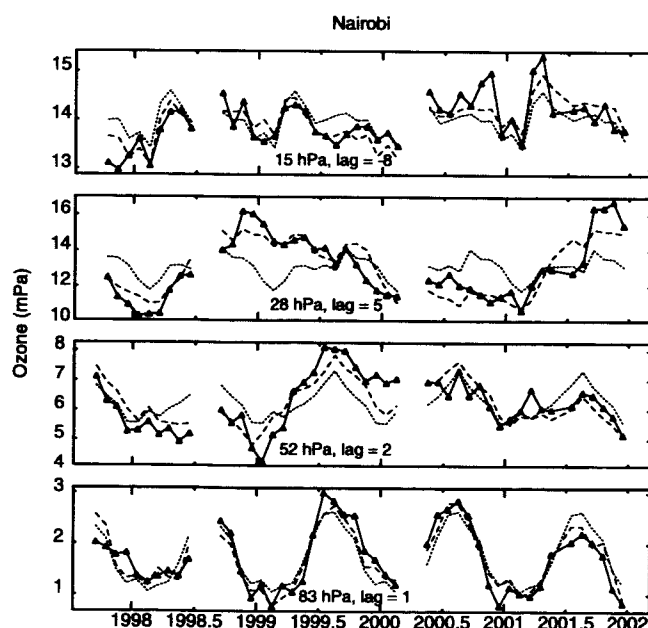


Figure 29. Comparison of the time series for ozone at Nairobi with the model fit. The data are shown by the solid line, the full model (equation (1)) with wind by the dashed line, and the model with the seasonal cycle only by the dotted line.

tion that the local ozone anomalies are largest during the descent of the shear zones (Figure 8).

[47] The QBO is seasonally synchronized near 20° , so we used a regression model that accounts for this for Samoa, Fiji, and Hilo, following the approach of *Randel and Wu* [1996] and *Wallace et al.* [1993]. We represented the QBO by the first two principal components of the deseasonalized Singapore zonal winds from 10 to 90 hPa for 1987–2000 for Hilo, and for 1995–2001 for Samoa and Fiji; the time projection of these components onto the wind anomalies gives the time series used in the model, Z_1 and Z_2 . The ozone time series at given pressure, $O_3(t)$, is then

$$O_3(t) = \sum_{i=1}^{12} \mu_i I_{i,t} + \sum_{j=1}^4 \gamma_{j1} I_{j,t} Z_1 + \sum_{j=1}^4 \gamma_{j2} I_{j,t} Z_2 + E_t \quad (2)$$

Here $I_{j,t}$ as an indicator series for season j of the year; $I_{j,t}$ is equal to 1 if t corresponds to season j (e.g., DJF) and zero otherwise; γ_{j1} and γ_{j2} are the associated seasonal coefficients for the QBO time series. We also fit the data with the seasonal cycle only, and fit the ozone anomalies with the two seasonal QBO terms.

[48] Figure 30 shows r^2 for the model fits to the ozone time series for Samoa and Hilo. The full model explains more than 60% of the variance for most of the profile for Samoa. The QBO terms are the largest contributor to the fit above 40 hPa, while the seasonal cycle dominates at lower altitudes. The fit to one of the QBO terms is significant in winter (or winter and spring), for all levels except for 25 hPa and 85 hPa. Figure 14 shows that 25 hPa is between the upper and middle ozone anomalies, so it is reasonable that the QBO fit is not significant there. Results for Fiji are similar, except that the model fit is somewhat better at most

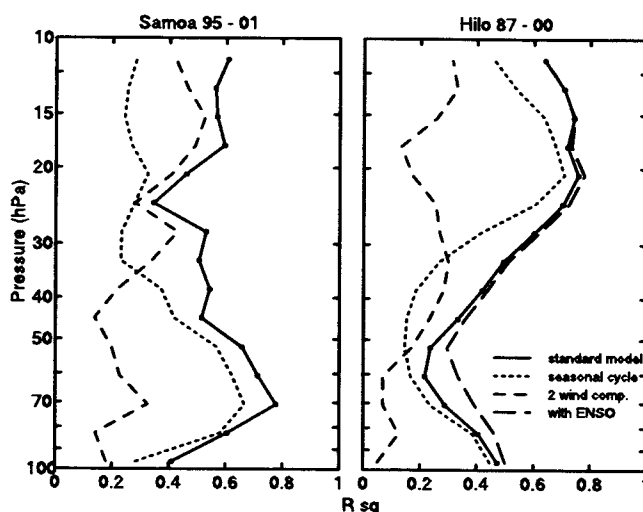


Figure 30. Vertical profile of R -squared for the regression model given by equation (2) for Samoa for 1995 to 2001 (left panel) and for Hilo, Hawaii, for 1987 to 2000 (right panel). The solid line gives r^2 for the full model and the dotted line gives the fit for the seasonal cycle only. The dashed line gives r^2 for fitting the monthly anomalies with the seasonal QBO terms. For Hilo, the long dashed lines gives r^2 for the model in equation (2) with the addition of a term for ENSO.

levels, but the time series is shorter. The QBO terms and the seasonal cycle terms contribute more equally at Fiji from 10 to 20 hPa than they do for Samoa.

[49] For Hilo, the model for 1987 to 2000 explains more than 60% of the variance from 10 to 30 hPa, but less than 40% from 45 to 75 hPa. In contrast to the picture for Samoa, the seasonal cycle is the largest contributor to the fit above 30 hPa and below 60 hPa, while the QBO terms and the seasonal cycle contribute about equally between 30 and 60 hPa. The fit to one or both of the QBO terms is significant in winter and spring at all levels from 10 to 45 hPa except 18–21 hPa. For Hilo, 20 hPa is between the upper and middle ozone anomalies (Figure 19). The QBO is the main contributor to the explained variance near 40 hPa, at the center of the lower QBO anomalies; however over half the variance is caused by factors other than the QBO and seasonal cycle.

[50] We added a term for a dependence on ENSO to equation (2), using the Nino-3 temperature anomalies (<http://ncep.noaa.gov>), and results of the fit with ENSO are shown by the long-dashed line in Figure 30. We found the best fit in the lower stratosphere by lagging ozone with respect to the ENSO term by 3 months, which is consistent with the strong correlation of ozone and temperature. The ENSO term was significant below 20 hPa, but it improved the explained variance only below 50 hPa, where ENSO is known to have an effect on stratospheric temperatures [Reid *et al.*, 1989]. The results in Figure 30 show that ENSO contributes more to explaining the variance of ozone below 50 hPa than does the QBO.

[51] We also added a term for the dependence of ozone on the solar cycle to equation (2); the solar cycle term was significant near 12 hPa, 20 hPa, and for 40–95 hPa. Including the solar cycle term changed the explained variance by less than 2% from 10 to 45 hPa, and by 3–6% from 50 to 95 hPa (not shown). The solar cycle term had less effect on the ozone variance than the ENSO term below 55 hPa.

[52] We ran the regression model for Hilo for 1994 to 2000, and found that it explains more than 80% of the variance from 10 to 30 hPa (with the seasonal fit dominating), about 40% for 50–60 hPa, and 65–75% elsewhere. The model is likely more successful for the shorter period in part because the relationship between the winds and the annual cycle is such as to favor a strong QBO effect at 20°N each winter/spring except one (1999–2000), as discussed above. The QBO fit is not significant in the lowest part of the stratosphere (70–95 hPa) for 1987–2000, but it is for the shorter period, 1994–2000.

[53] The regression model accounting for only the seasonal cycle and the QBO effects provides a better fit to the data for Samoa and Fiji than for Hilo in the lower stratosphere, and this is likely because other factors influence ozone more over Hilo. Hilo is in a more dynamically active location, with more mid-latitude influence than either Samoa and Fiji, as shown for example by *Waugh and Polvani* [2000]. In the lower stratosphere, mean ozone concentrations are higher over Hilo than over Samoa and Fiji in the corresponding season (see Figure 18). They are also more variable, particularly in local winter and spring, as shown by the cumulative probability plots in Figure 31. Median values of ozone are similar in local winter for the

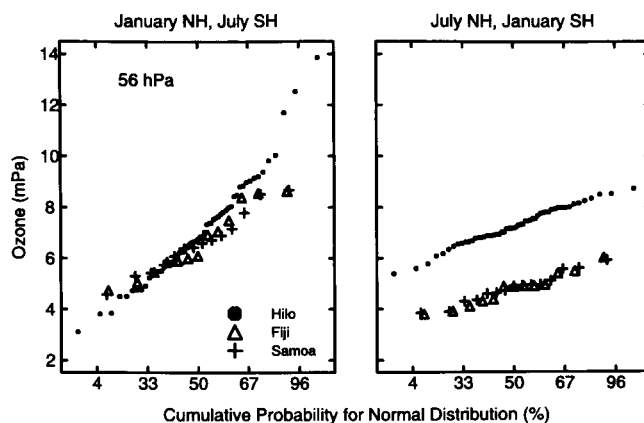


Figure 31. Cumulative probability distribution for ozone at 56 hPa for Hilo, Samoa, and Fiji, plotted against a normal distribution. The concentrations for each station are arranged in order of ascending magnitude; normally distributed data define a straight line in this type of plot.

three stations, but Hilo shows a tail of high values that are lacking at Samoa and Fiji. Inspection of individual profiles shows layers of high ozone below 30 hPa over Hilo between January and April, a feature not present in any month at the southern tropical stations considered here. The distributions of ozone in the two hemispheres are more similar in local summer, except that values are significantly higher near 20°N than near 20°S.

6. Summary and Discussion

[54] Analysis of the first in situ equatorial ozone profiles has revealed the dramatic changes in the shape of the profiles caused by the QBO, with the partial pressure maximum increasing by ~25% in 5–6 months, as it descends from 17.5 to 24 hPa, or by ~2 km. The most dramatic change in shape accompanies the descent of the westerly shear zones. The sonde data, with their simultaneous measurements, reveal clearly the strong association of ozone and temperature below 15 hPa. The amplitude of the QBO in ozone in the lower stratosphere exceeds $\pm 20\%$ at 30 hPa (24 km). This is much larger than indicated by previous analyses of SAGE II data [Zawodny and McCormick, 1991; Hasebe, 1994; Randel and Wu, 1996], likely because these analyses averaged over several degrees of latitude. Our analysis of the reprocessed SAGE II data gives a somewhat smaller amplitude than the sonde data, for a narrow latitude band (2°N–2°S); the smaller amplitude is likely a consequence of the lower vertical resolution of the SAGE data, as well as the interpolation and smoothing required by the data record. The sonde data reveal the descent of the QBO in ozone to lower altitudes than was possible with the earlier version of SAGE II data, with an amplitude exceeding $\pm 20\%$ at 80 hPa (18 km). The linear regression model indicates that the fit to the QBO is significant as low as 95 hPa, but the record includes only two QBO cycles. The temperatures below 50 hPa are strongly influenced by ENSO in northern winter as well as by the QBO [Reid, 1994], and the sonde and SAGE data show that the major warm phase in 1997/98 interrupted what otherwise would have been a positive

ozone anomaly in the lower stratosphere. Reid [1994] shows that the ENSO and QBO effects on temperature can either reinforce or cancel in the lower stratosphere. The 16-year SAGE record indicates clearly that this is the case for ozone also. Equatorial ozone values are influenced primarily by the QBO between about 20 and 45 hPa, while the seasonal cycle is more important below 50 hPa; the two contribute about equally from 10 to 15 hPa.

[55] The equatorial and subtropical ozone data both show an upper and lower band of QBO anomalies. The cross over between these is at a higher altitude for the equator than for the subtropics, 14 hPa (29 km) versus 22 hPa (26 km). This is consistent with the switch from dynamical control to chemical control occurring at a slightly lower altitude in the subtropics, as shown by the model calculations of Chipperfield and Gray [1992].

[56] Previous analyses of SAGE II data from the 1980s indicated that the QBO anomalies in the lower stratosphere near 20° are usually out of phase with those over the equator. The sonde and SAGE II data from the 1990s show that this is not always the case. In particular, we find that the ozone anomaly at 20°S lags that at the equator by only a few months during the easterlies from 1994 to 1998, contrary to the previous picture of the subtropical and equatorial anomalies being out of phase. The timing of the equatorial winds with respect to the annual cycle near 35 hPa during much of the 1990s favored strong ozone anomalies in the northern subtropics that are out of phase with those on the equator, but did not favor strong anomalies in the southern subtropics. Randel *et al.* [1999] found that the anomalies in the residual mean vertical velocities at 32 hPa in the northern subtropics were out of phase with those over the equator in 1992–1998. However, in austral fall of 1994, 1996, and 1998, the residual vertical velocities in the southern subtropics are in phase with those over the equator, consistent with the ozone signal.

[57] Recent analyses of CH₄ data showed that the QBO at 12 hPa was also much stronger in the northern than in the southern subtropics from 1993 to 1999, based on data from UARS (the Upper Atmosphere Research Satellite) [Dunkerton, 2001]. The QBO signal in ozone from 27 to 35 km is also stronger at 20°N than at 20°S for most years from 1993 to 1999. The relatively short record from UARS is biased in its sampling of the phase relationship between the QBO and the annual cycle compared to the longer record from SAGE II, especially since the QBO was essentially biennial for two cycles from 1994 to 1998.

[58] Hofmann *et al.* [1996] noted empirically that the winters with lowest column ozone over Mauna Loa, Hawaii, are those when the winds change from easterly to westerly at 30 hPa a few months earlier. Ozone values in the winter of 1994–1995 were the lowest on record. The sonde data from Hilo show that during this winter, there were negative ozone anomalies from 8 hPa down to 80 hPa (Figures 19 and 25a), a feature which has not occurred at any other time from 1985 to 2000. While the low values down to 50 hPa are likely caused by the QBO, the low values at the lower altitudes are likely a result of the warm ENSO phase at that time.

[59] We find that there is often a three-cell structure in the subtropical ozone anomalies, with the anomalies above 20 hPa (27 km) and from 50 to 20 hPa (20–27 km) related to

the QBO, while the anomalies below 50 hPa are often related to ENSO. Both anomalies above 50 hPa can be important for the QBO in column ozone, as they are below and above the partial pressure maximum (~20 hPa); in contrast, over the equator, the lower band of anomalies dominates the QBO signal in column ozone because it includes the partial pressure maximum, while the upper anomalies starts well above the maximum, where ozone concentrations are lower.

[60] There is a strong anomaly in subtropical column ozone (>5 DU, or 2%) when the anomalies above 20 hPa and those from 50 to 20 hPa reinforce one another. There were four strong column anomalies at 20°N and 20°S from 1985 to 1991. However, there were many more strong column anomalies in the northern subtropics from 1993 to 1999 compared to the southern subtropics, five versus one respectively. We find that 70% of the cases with a strong column signal in winter/spring are associated with strong shear at 25–35 hPa in the late fall/early winter. Conversely, 75% of the cases with strong shear at these levels are associated with a strong column signal. It is expected that the QBO-related ozone anomalies in the lower and middle stratosphere are of the same sign when the strong shear is located in the lower stratosphere, given the QBO-induced circulation and its effects on ozone as a dynamical tracer below about 28 km and on NO_y above.

[61] Weak anomalies in column ozone (<5 DU) in the subtropics typically occur when the ozone anomalies above and below 20 hPa are either of opposite sign, or one of them is very small. Over half of these cases (60%) are associated with strong wind shear in late fall/early winter in the middle stratosphere at 12.5 hPa. In the southern subtropics, there is strong shear at 12.5 hPa and a weak column ozone anomaly for five of six years from 1994 to 1999.

[62] Baldwin *et al.* [2001] commented on years with a missing subtropical anomaly based on a statistical fit to monthly anomalies in column ozone (their Figure 21). The years with no apparent subtropical anomaly are not always the same for the original time series of anomalies as for the QBO component derived by seasonally varying regression. This may well be because the regression model for the column cannot account for two features present in the middle and lower stratosphere that cancel out. It may also be because the atmospheric response to the QBO cannot be simulated well by the statistical fit to the equatorial winds, but the cancellation obviously causes an added complication.

[63] We found that the factors contributing to the variance in ozone were different for 20°N and 20°S. Above the partial pressure maximum, where the ozone lifetime is relatively short, the seasonal cycle is more important than the QBO near 20°N, while the QBO appears to be somewhat more important than the seasonal cycle near 20°S. The seasonal cycle dominates the variance in ozone below 40 hPa near 20°S, and explains much more of the variance in the lower stratosphere than it does near 20°N. The regression model for Hilo indicate that the effects of ENSO have more effect on ozone below 60 hPa than does the QBO. However, other factors not considered here, such as transport of ozone from mid-latitudes, are clearly important for Hilo below 30 hPa. It may be that longer time series from the southern subtropics will modify the results sum-

marized here, but the conclusions regarding the seasonal cycle and the QBO for Hilo hold true whether 6 years of 15 years of data are used in the analysis.

[64] **Acknowledgments.** This work was funded with support from the National Aeronautics and Space Administration's Atmospheric Chemistry Modeling and Data Analysis Program, including grant NAG1-2025 to Harvard University. We thank Anne Thompson for her efforts in bringing the SHADOZ network into being, allowing the rapid dissemination of the ozonesonde data, and Jacquelyn Witte for her able management of the SHADOZ web site. We would also like to thank Bruno Hoegger and Gilbert Levrat from Payeme, Switzerland, who worked with the Kenya Department of Meteorology to develop and sustain the Nairobi ozone sonde station. We thank Barbara Naujokat for providing the equatorial wind data. Tim Dunkerton provided a very helpful review that led to a much improved analysis of the subtropical QBO in column ozone.

References

- Baldwin, M. P., et al., The quasi-biennial oscillation, *Rev. Geophys.*, **39**, 179–229, 2001.
- Bowman, K. P., Global patterns of the quasi-biennial oscillation in total ozone, *J. Atmos. Sci.*, **46**, 3328–3343, 1989.
- Chipperfield, M. P., and L. J. Gray, Two-dimensional model studies of the interannual variability of trace gases in the middle atmosphere, *J. Geophys. Res.*, **97**, 5963–5980, 1992.
- Chipperfield, M. P., L. J. Gray, J. S. Kinnersley, and J. Zawodny, A two-dimensional model study of the QBO signal in SAGE II NO₂ and O₃, *Geophys. Res. Lett.*, **21**, 589–592, 1994.
- Cunnold, D. M., H. J. Wang, L. Thomason, J. Zawodny, J. A. Logan, and I. A. Megretskaja, SAGE (version 5.96) ozone trends in the lower stratosphere, *J. Geophys. Res.*, **105**, 4445–4457, 2000.
- Dunkerton, T. J., The role of gravity waves in the quasi-biennial oscillation, *J. Geophys. Res.*, **102**, 26,053–26,076, 1997.
- Dunkerton, T. J., Quasi-biennial and subbiennial variation of stratospheric trace constituents derived from HALOE observations, *J. Atmos. Sci.*, **58**, 7–25, 2001.
- Fujiwara, M., F. Hasebe, M. Shiotani, N. Nishi, H. Vömel, and S. J. Oltmans, Water vapor control at the tropopause by equatorial Kelvin waves observed over the Galapagos, *Geophys. Res. Lett.*, **28**, 3143–3146, 2001.
- Garcia, R. R., and S. Solomon, The effect of breaking gravity waves on the dynamics and chemical composition of the mesosphere and lower thermosphere, *J. Geophys. Res.*, **90**, 3850–3868, 1985.
- Gray, L. J., and T. J. Dunkerton, The role of the seasonal cycle in the quasi-biennial oscillation of ozone, *J. Atmos. Sci.*, **47**, 2429–2451, 1990.
- Gray, L. J., and S. Ruth, The modeled latitudinal distribution of the ozone quasi-biennial oscillation using observed equatorial winds, *J. Atmos. Sci.*, **50**, 1033–1046, 1993.
- Hamilton, K., Interhemispheric asymmetry and annual synchronization of the ozone quasi-biennial oscillation, *J. Atmos. Sci.*, **46**, 1019–1025, 1989.
- Hasebe, F., Quasi-biennial oscillations of ozone and diabatic circulation in the equatorial stratosphere, *J. Atmos. Sci.*, **51**, 729–754, 1994.
- Hofmann, D. J., S. J. Oltmans, J. M. Harris, W. D. Komhyr, J. A. Lathrop, T. DeForr, and F. Kuniyuki, Ozonesonde measurements at Hilo, Hawaii, following the eruption of Pinatubo, *Geophys. Res. Lett.*, **20**, 1533–1536, 1993.
- Hofmann, D. J., et al., Record low ozone at Mauna Loa Observatory during winter 1994–1995: A consequence of chemical and dynamical synergism?, *Geophys. Res. Lett.*, **23**, 1533–1536, 1996.
- Hollandsworth, S. M., K. P. Bowman, and R. D. McPeters, Observational study of the quasi-biennial oscillation in ozone, *J. Geophys. Res.*, **100**, 7347–7361, 1995.
- Holton, J. R., and R. S. Lindzen, An updated theory for the quasi-biennial cycle of the tropical stratosphere, *J. Atmos. Sci.*, **29**, 1076–1080, 1972.
- Johnson, B. J., S. J. Oltmans, H. Vömel, H. G. J. Smit, T. Deschler, and C. Kroger, Electrochemical concentration cell (ECC) ozonesonde pump efficiency measurements and tests on the sensitivity to ozone of buffered and unbuffered ECC sensor solutions, *J. Geophys. Res.*, **107**(D19), 4393, doi:10.1029/2001JD000557, 2002.
- Jones, D. B. A., H. R. Schneider, and M. B. McElroy, Effects of the quasi-biennial oscillation on the zonally averaged transport of tracers, *J. Geophys. Res.*, **103**, 11,235–11,249, 1998.
- Kinnersley, J. S., On the seasonal asymmetry of the lower and middle latitude QBO circulation anomaly, *J. Atmos. Sci.*, **56**, 1942–1962, 1999.
- Lait, L. R., M. R. Schoeberl, and P. A. Newman, Quasi-biennial modulation of Antarctic ozone depletion, *J. Geophys. Res.*, **94**, 11,559–11,571, 1989.
- Leblanc, T., and I. S. McDermid, Quasi-biennial oscillation signatures in ozone and temperature observed by lidar at Mauna Loa Observatory, Hawaii (19.5°N, 155.6°W), *J. Geophys. Res.*, **106**, 14,869–14,874, 2001.
- Lindzen, R. S., and J. R. Holton, A theory of the quasi-biennial oscillation, *J. Atmos. Sci.*, **25**, 1095–1107, 1968.
- Ling, X.-D., and J. London, The quasi-biennial oscillation of ozone in the tropical middle stratosphere: A one-dimensional model, *J. Atmos. Sci.*, **43**, 3122–3136, 1986.
- Logan, J. A., An analysis of ozonesonde data for the lower stratosphere: Recommendations for testing models, *J. Geophys. Res.*, **104**, 16,151–16,170, 1999.
- McCormick, M. P., J. M. Zawodny, R. E. Veiga, J. C. Larsen, and P. H. Wang, An overview of SAGE I and II ozone measurements, *Planet. Space Sci.*, **37**, 1567–1586, 1989.
- McPeters, R. D., G. J. Labow, and B. J. Johnson, A satellite-derived ozone climatology for balloonsonde estimation of total column ozone, *J. Geophys. Res.*, **102**, 8875–8885, 1997.
- Naujokat, B., An update of the observed quasi-biennial oscillation of the stratospheric winds over the tropics, *J. Atmos. Sci.*, **43**, 1873–1877, 1986.
- Oltmans, S. J., and J. London, The quasi-biennial oscillation in atmospheric ozone, *J. Geophys. Res.*, **87**, 8981–8989, 1982.
- Oltmans, S. J., et al., Ozone in the Pacific troposphere from ozonesonde observations, *J. Geophys. Res.*, **106**, 32,503–32,525, 2001.
- Randel, W. J., and F. Wu, Isolation of the ozone QBO in SAGE II data by singular decomposition, *J. Atmos. Sci.*, **53**, 2546–2559, 1996.
- Randel, W. J., F. Wu, R. Swinbank, J. Nash, and A. O'Neill, Global QBO circulation derived from UKMO stratospheric analyses, *J. Atmos. Sci.*, **56**, 457–474, 1999.
- Randel, W. J., F. Wu, and D. J. Gaffen, Interannual variability of the tropical tropopause derived from radiosonde data and NCEP reanalyses, *J. Geophys. Res.*, **105**, 15,509–15,523, 2000.
- Reed, R. J., A tentative model of the 26-month oscillation in tropical latitudes, *Q. J. R. Meteorol. Soc.*, **90**, 441–466, 1964.
- Reed, R. J., W. J. Campbell, L. A. Rasmussen, and R. G. Rogers, Evidence of a downward propagating annual wind reversal in the equatorial stratosphere, *J. Geophys. Res.*, **66**, 813–818, 1961.
- Reid, G. C., Seasonal and interannual temperature variations in the tropical stratosphere, *J. Geophys. Res.*, **99**, 18,923–18,932, 1994.
- Reid, G. C., K. S. Gage, and J. R. McAfee, The thermal response of the tropical atmosphere to variations in equatorial Pacific sea surface temperature, *J. Geophys. Res.*, **94**, 14,705–14,716, 1989.
- Thompson, A. M., et al., Southern Hemisphere Additional Ozonesondes (SHADOZ) 1998–2000 tropical ozone climatology: I. Comparison with Total Ozone Mapping Spectrometer (TOMS) and ground-based measurements, *J. Geophys. Res.*, **108**(D2), 8238, doi:10.1029/2001JD000967, 2003.
- Wallace, J. M., R. L. Panetta, and J. Estberg, Representation of the equatorial stratospheric quasi-biennial oscillation in EOF phase space, *J. Atmos. Sci.*, **50**, 1751–1761, 1993.
- Wang, H. J., D. M. Cunnold, L. W. Thomason, J. M. Zawodny, and G. E. Bodeker, Assessment of SAGE version 6.1 ozone data quality, *J. Geophys. Res.*, **107**(D23), 4691, doi:10.1029/2002JD002418, 2002.
- Waugh, D. W., and L. M. Polvani, Climatology of intrusions into the tropical upper troposphere, *Geophys. Res. Lett.*, **27**, 3857–3860, 2000.
- World Meteorological Organization (WMO), Assessment of trends in the vertical distribution of ozone, *SPARC Rep. 1*, WMO-Ozone Res. and Monit. Proj. Rep. 43, Geneva, 1998.
- Zawodny, J. M., and M. P. McCormick, Stratospheric Aerosol and Gas Experiment II: Measurements of the quasi-biennial oscillation in ozone and nitrogen dioxide, *J. Geophys. Res.*, **96**, 9371–9377, 1991.

W. Kimani, Kenya Meteorological Department, Box 30259, Nairobi, Kenya.

B. J. Johnson, S. J. Oltmans, and H. Vömel, Climate and Diagnostic Laboratory, NOAA, 325 Broadway, Mail Code R/E/CG1, Boulder, CO 80303, USA.

D. B. A. Jones, J. A. Logan, and I. A. Megretskaja, Department of Earth and Planetary Sciences, Harvard University, 29 Oxford Street, Cambridge, MA 02138, USA. (jal@io.harvard.edu)

W. J. Randel, Atmospheric Chemistry Division, National Center for Atmospheric Research, 1850 Table Mesa Drive, Boulder, CO 80307, USA.

F. J. Schmidlin, Observational Science Branch, NASA Wallops Flight Facility, Wallops Island, VA 23337, USA.